

# Hidden On-Shell Mediators for the Galactic Center $\gamma$ -ray Excess

Mohammad Abdullah<sup>a</sup>, Anthony DiFranzo<sup>b</sup>, Arvind Rajaraman<sup>c</sup>,  
Tim M. P. Tait<sup>d</sup>, Philip Tanedo<sup>e</sup>, Alexander M. Wijangco<sup>f</sup>,

*Department of Physics & Astronomy, University of California, Irvine, CA 92697*

## Abstract

We present simplified models for the galactic center  $\gamma$ -ray excess where Dirac dark matter annihilates into pairs or triplets of on-shell bosonic mediators to the Standard Model. These annihilation modes allow the dark matter mass to be heavier than those of conventional effective theories for the  $\gamma$ -ray excess. Because the annihilation rate is set by the dark matter–mediator coupling, the Standard Model coupling can be made parametrically small to ‘hide’ the dark sector by suppressing direct detection and collider signals. We explore the viability of these models as a thermal relic and on the role of the mediators for controlling the  $\gamma$ -ray spectral shape. We comment on ultraviolet completions for these simplified models and novel options for Standard Model final states.

INTRODUCTION . . . . .	1
ON-SHELL SIMPLIFIED MODELS . . . . .	5
THE $\gamma$ -RAY EXCESS FROM ON-SHELL MEDIATORS . . . . .	9
EXPERIMENTAL BOUNDS ON THE SM COUPLING . . . . .	12
VIABILITY AS A THERMAL RELIC . . . . .	15
COMMENTS ON UV COMPLETIONS AND MODEL BUILDING . . . . .	18
CONCLUSIONS AND OUTLOOK . . . . .	21
THE SPECTRUM OF SPECTRA . . . . .	22

## 1 Introduction

The particle nature of dark matter (DM) remains one of the outstanding open questions in high energy physics. Experimental probes of the dynamics that connect the dark sector and the Standard Model (SM) fall into three complimentary classes shown schematically in Fig. 1 See [1] for a status report.

Recent analyses of the FERMI Space Telescope data find an excess of 1–10 GeV  $\gamma$ -rays from the center of the galaxy. In fact, a similar excess seems to extend away from the center to high galactic latitudes [2–4]. This may be indicative of dark matter annihilating into SM final states which later shower to produce the observed excess photon spectrum [5–15]; see [15–24] for recent models. While an early estimate argued that an alternate interpretation based on unidentified millisecond pulsars is unlikely [25], [13] and [26] recently demonstrated the consistency of this hypothesis with the  $\gamma$ -ray excess. Indeed, it may be difficult to distinguish these two possibilities since the extrapolated millisecond pulsar (MSP) profile is very similar to standard DM profiles [27]. For the remainder of this paper we assume the excess is generated by DM annihilation. The latest

---

<sup>a</sup>maabdull@, <sup>b</sup>adifranz@, <sup>c</sup>arajaram@, <sup>d</sup>ttait@, <sup>e</sup>flip.tanedo@, <sup>f</sup>awijangco@uci.edu

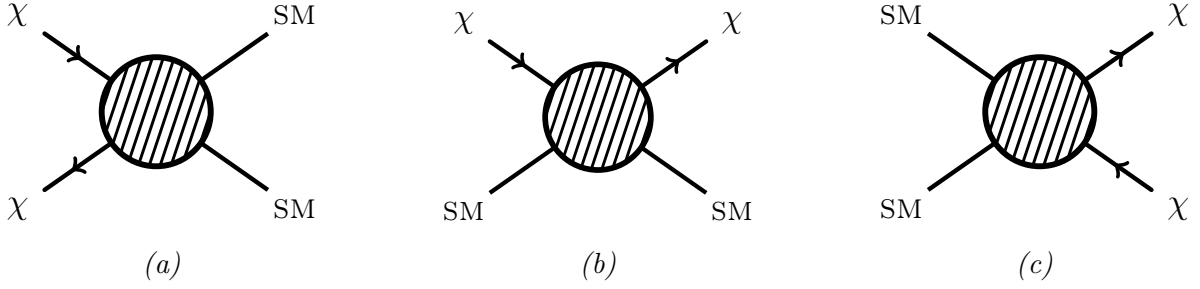


Figure 1: (a) Annihilation, (b) Direct Detection, (c) Collider. Complimentary modes of dark matter detection. Annihilation sets both the thermal relic abundance and the present-day indirect detection rate.

analyses prefer a 40 GeV dark matter candidate that annihilates into  $b\bar{b}$  pairs<sup>1</sup> with a thermally averaged cross section  $\langle\sigma v\rangle_{b\bar{b}} \approx \mathcal{O}(\text{few}) \times 10^{-26} \text{cm}^3/\text{s}$  [13, 14]. Further, because  $\langle\sigma v\rangle_{b\bar{b}}$  is close to the value required to be a thermal relic from standard freeze-out, it is implausible that such a relic could produce such a  $\gamma$ -ray signal without having an  $s$ -wave annihilation mode. Combined with constraints from direct detection and collider experiments, this signal motivates a more detailed study of the physics encoded in the shaded regions of Fig. 1.

## 1.1 From Effective Theories to Simplified Models

A simple parameterization of the SM–DM interaction is to treat the shaded blobs as effective contact interactions between dark matter particles ( $\chi$ ) and SM states. For example, the coupling of fermionic DM to a quark  $q$  is parameterized through nonrenormalizable operators

$$\mathcal{L} \supset \frac{1}{\Lambda^2} (\bar{\chi} \mathcal{O}_\chi \chi) (\bar{q} \mathcal{O}_q q), \quad (1.1)$$

where, for example,  $\mathcal{O}_\chi \otimes \mathcal{O}_q = \gamma^\mu \otimes \gamma_\mu$  corresponds to an interaction mediated by a heavy vector mediator that has been integrated out. The coefficient  $\Lambda^{-2}$  can be calculated for specific DM models and allow one to apply bounds from different types of experiments in a model-independent way. This technique has been applied, for example, for collider [32–52], indirect detection [42, 53–60] and direct detection [61–69] bounds on dark matter. The choice of pairwise dark matter interactions assumes the existence of a symmetry that also stabilizes the DM particle against decay while the pairwise SM interactions are assumed to be the leading order gauge-invariant operators. This need not be the case as has been demonstrated for annihilation [70] and direct detection [71]. In these cases, the structure in (1.1) fails to capture the physics of the mediator fields which couple to both the dark and visible (SM) sectors: the effective contact interaction description breaks down when the mediators do not decouple. The limitations of the contact interaction bounds were pointed out in [35] and highlighted in [72–75].

This motivates a shift in the *lingua franca* used to compare experimental results to models: rather than contact interactions, light (nondecoupled) mediators suggest using ‘simplified models’ that include the renormalizable dynamics of the mediator fields [76]. This approach has been applied to colliders [73–75, 77–87] and astrophysical bounds where the physics of the mediator has been explored in DM self-interactions [88–107].

<sup>1</sup>Annihilation of 10 GeV DM into  $\tau\bar{\tau}$  is also plausible fit, see [18, 19, 22, 28–30] for recent models. [31] found that a universal coupling to charged leptons may be favored after bremsstrahlung and inverse Compton scattering effects are included. In this paper we focus on the case where the  $\gamma$ -ray excess is generated by  $b\bar{b}$  pairs; we comment on more general final states in Section 6.1 and Appendix A.

Name	Operator	Constraint
D2	$(\bar{\chi}\gamma_5\chi)(\bar{q}q)$	Edge of EFT validity from monojet bounds
D4	$(\bar{\chi}\gamma_5\chi)(\bar{q}\gamma_5q)$	Edge of EFT validity from monojet bounds
D5	$(\bar{\chi}\gamma^\mu\chi)(\bar{q}\gamma_\mu q)$	Spin independent direct detection
D6	$(\bar{\chi}\gamma^\mu\gamma_5\chi)(\bar{q}\gamma_\mu q)$	Related to D5, D8 in chiral basis
D7	$(\bar{\chi}\gamma^\mu\chi)(\bar{q}\gamma_\mu\gamma_5q)$	Related to D5, D8 in chiral basis
D8	$(\bar{\chi}\gamma^\mu\gamma_5\chi)(\bar{q}\gamma_\mu\gamma_5q)$	Spin dependent direct detection
D9	$(\bar{\chi}\sigma^{\mu\nu}\chi)(\bar{q}\sigma_{\mu\nu}q)$	Nontrivial spin-2 UV completion
D10	$(\bar{\chi}\sigma^{\mu\nu}\gamma^5\chi)(\bar{q}\sigma_{\mu\nu}q)$	Nontrivial spin-2 UV completion
D12	$(\bar{\chi}\gamma_5\chi)G_{\mu\nu}G^{\mu\nu}$	Monojet bounds
D14	$(\bar{\chi}\gamma_5\chi)G_{\mu\nu}\tilde{G}^{\mu\nu}$	Monojet bounds

Table 1: Contact operators between Dirac DM and quarks or gluons [36] that support  $s$ -wave annihilation and the constraint for the galactic center. See [108] for a recent technical analysis.

## 1.2 The $\gamma$ -ray Excess Suggests Light Mediators

When the galactic center signal is combined with complementary bounds from direct detection and colliders, one is generically led to the limit where the contact interaction description (1.1) breaks down and a simplified model description is necessary. By ‘generic’ we mean no parameter tuning or additional model building is invoked.

The tension is summarized in Table 1, where we list the Dirac fermion dark matter contact interactions that satisfy the requirement of  $s$ -wave annihilation<sup>2</sup>. Because each effective operator simultaneously encodes the various DM–SM interactions in Fig. 1, requiring a coupling large enough to produce the  $\gamma$ -ray excess automatically generates signals that are constrained by null results at direct detection [109, 110] and monojet [111] experiments. These rule out operators D5, D8, D12, and D14 in Table 1. The operators D2 and D4 are at the edge of the validity of the effective theory [73–75]. We ignore the D9 and D10 operators since they cannot be UV completed by a renormalizable theory. Finally, the D6 and D7 operators are related to D5 and D8 by the chiral structure of the Standard Model. The fermionic  $SU(2)_L \times U(1)_Y$  eigenstates are chiral so that gauge invariant interactions are naturally written in a chiral basis  $\bar{q}\mathcal{O}_q P_{L,R}q$  where  $P_{L,R} = \frac{1}{2}(1 \mp \gamma^5)$ . Thus one generically expects that in the absence of tuning<sup>3</sup>, the presence of vector or axial couplings implies the existence of the other.

It is thus difficult to account for the  $\gamma$ -ray excess in the ‘heavy mediator’ limit where these contact interactions are valid. A more technical analysis of the contact interaction description was recently performed in [56, 108, 112] and includes the case of scalar dark matter. The  $\gamma$ -ray excess thus generically implies a dark sector with mediators that do not decouple and hence is more accurately described in a simplified model framework. Recent comprehensive studies of simplified models for the  $\gamma$ -ray excess have dark matter annihilating through off-shell mediators ( $s$ - and  $t$ -channel diagrams) [113, 114]; see [115, 116] for an earlier model.

<sup>2</sup>Majorana dark matter relaxes these bounds by forcing some of these operators to vanish identically.

<sup>3</sup>It is worth noting that such a ‘coincidental’ cancellation occurs in the  $Z$  coupling to charged leptons which is dominantly axial due to  $\sin^2\theta_W \approx 1/4$ .

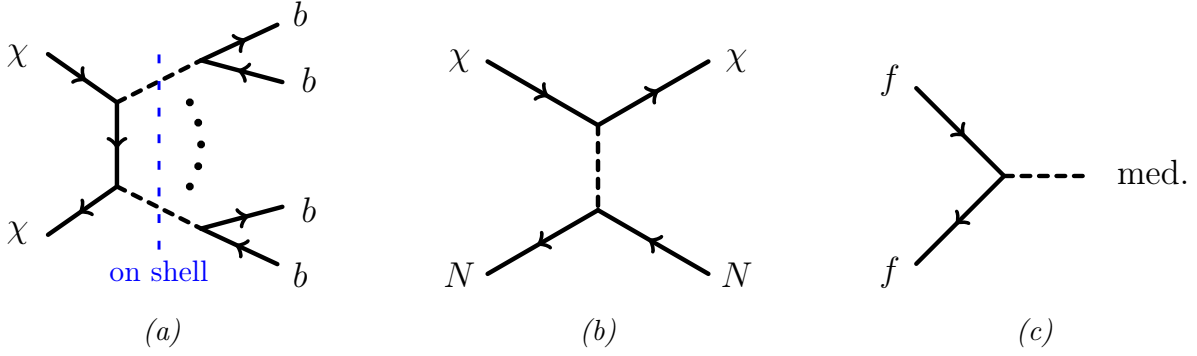


Figure 2: (a) Annihilation, (b) Direct Detection, (c) Collider. DM complementarity for on-shell mediators; compare to Fig. 1. (a) The annihilation rate is independent of the mediator coupling to the Standard Model. (b) Direct detection remains 2-to-2, here  $N$  is a target nucleon. (c) Colliders can search for the presence of the mediator independently of its DM coupling.

### 1.3 Annihilation to On-shell Mediators

In this paper we focus on a different region in the space of simplified models where mediators are light enough that they can be produced on-shell in dark matter annihilation, henceforth referred to as the on-shell mediator scenario. This annihilation mode is largely independent of the mediator’s coupling to the SM so long as the latter is nonzero. Lower limits on the SM coupling—that is, upper limits on the mediator lifetimes—are negligible since the mediator may propagate astrophysical distances before decaying to the  $b\bar{b}$  pairs that subsequently yield the  $\gamma$ -ray excess. The SM coupling can be parametrically small which suppresses the off-shell  $s$ -channel annihilation mode as well as the direct detection and collider signals. This is shown in Fig. 2.

Because on-shell annihilation into mediators requires at least two final states<sup>4</sup>, the resulting annihilation produces at least four  $b$  quarks, as shown in Fig. 2a. This, in turn, requires a heavier dark matter mass in order to eject  $\approx 40$  GeV  $b$  quarks from each annihilation to fit the  $\gamma$ -ray excess. This avoids the conventional wisdom that this excess requires 10 – 40 GeV dark matter. In the limit on-shell annihilation dominates, the total excess  $\gamma$ -ray flux is fit by a single parameter, the mediator coupling to dark matter. Once fit, this parameter determines whether the DM may be a thermal relic. We remark that the spectrum is slightly boosted by the on-shell mediator; we address this below and explore possibilities where the mediator mass can be used as a handle to change the spectral features.

The on-shell mediator limit thus separates the physics of mediators SM and DM couplings. The former can be made parametrically small to hide DM from direct detection and collider experiments, while the latter can be used to independently fit indirect detection signals such as the galactic center  $\gamma$ -ray excess. Observe that these simplified models modify the standard picture of complementary DM searches for contact interactions shown schematically in Fig. 2. Annihilation now occurs through multiple mediator particles and is independent of the mediator coupling to the SM. Direct detection proceeds as usual through single mediator exchange between DM and SM. Collider bounds, on the other hand, need not depend on the DM coupling at all and can focus on detecting the mediator rather than the dark matter missing energy.

In this paper we explore the phenomenology of on-shell mediator simplified models for the galactic center. This paper is organized as follows. In the following two sections we present the

<sup>4</sup>One may also consider semi-annihilation processes  $\chi_1\chi_2 \rightarrow \chi_3(\text{mediator})$  [117]. See [118] for a prototype model for the galactic center  $\gamma$ -ray excess.

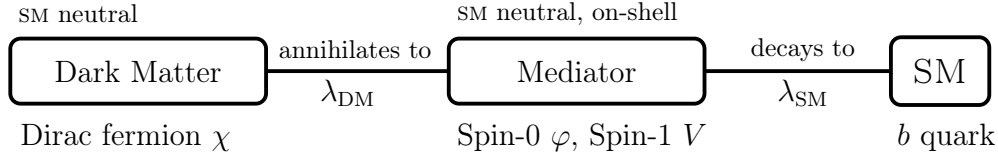


Figure 3: Dark matter annihilates to on-shell mediators, which in turn decay into  $b\bar{b}$  pairs. Each step is controlled by a separate coupling,  $\lambda$ . See text for details.

on-shell simplified models that generate the  $\gamma$ -ray excess and determine the range of dark sector parameters. We then assess in Section 4 the extent to which the on-shell mediators must be parametrically hidden from direct detection and colliders. In Section 5 we discuss the viability of this scenario for thermal relics. We comment on the lessons for UV models of dark matter in Section 6. Appendix A briefly describes plausible variants for generating  $\gamma$ -ray spectra with more diverse SM final states.

## 2 On-Shell Simplified Models

Fig. 3 schematically represents the class of simplified models that we consider. We assume the existence of a single SM neutral spin-0 or spin-1 mediator which couples to Dirac fermion DM with coupling  $\lambda_{\text{DM}}$  and  $b\bar{b}$  pairs with coupling  $\lambda_{\text{SM}}$ . Majorana fermions do not differ qualitatively in this regime. We focus on the case where mediators couple to the Dirac DM fermion with coupling  $\lambda_{\text{DM}}$  and to  $b\bar{b}$  pairs with coupling  $\lambda_{\text{SM}}$ .

### 2.1 Parity Versus Chirality

Before describing the mediator interactions, we remark on the utility of the parity and chirality bases for four-component fermion interactions. In the parity basis, one uses explicit factors of the  $\gamma^5$  matrix to parameterize

$$\text{scalar } (\mathbb{1}), \quad \text{pseudoscalar } (\gamma^5), \quad \text{vector } (\gamma^\mu), \quad \text{and axial } (\gamma^\mu \gamma^5). \quad (2.1)$$

interactions. This basis is most suited for nonrelativistic interactions. Equivalently, in the chirality basis, one inserts chiral projection operators  $P_{L,R} = \frac{1}{2}(1 \mp \gamma^5)$  into fermion bilinears. This is the natural description of SM gauge invariants. The spin-0 fermion bilinears are

$$\bar{\Psi}(\mathbb{1}, \gamma^5)\Psi = \bar{\Psi}P_L\Psi \pm \bar{\Psi}P_R\Psi = \psi\chi \mp \text{h.c.} \quad (2.2)$$

where we have written the Dirac spinor in terms of two-component left-handed Weyl spinors  $\Psi = (\psi, \chi^\dagger)^T$ , see e.g. [119]. Similarly, the spin-1 bilinears are

$$\bar{\Psi}\gamma^\mu(\mathbb{1}, \gamma^5)\Psi = \bar{\Psi}\gamma^\mu P_L\Psi \pm \bar{\Psi}\gamma^\mu P_R\Psi = \psi^\dagger \bar{\sigma}^\mu \psi \mp \chi^\dagger \bar{\sigma}^\mu \chi. \quad (2.3)$$

The  $\gamma^5$  appears as a phase in the spin-0 coupling and a relative sign in the spin-1 couplings of opposite chirality fermions.

The phenomenology of the  $\gamma$ -ray excess suggests the use of both descriptions. DM annihilation and direct detection occur nonrelativistically so the choice of a scalar (vector) versus a pseudoscalar (axial) can dramatically affect the rate for these processes. It is thus useful to parameterize these

Interaction	S (P)	V (A)	S (P)	V (A)	S (P)	V (A)
Partial Wave	$p$ ( $s$ )	$s$ ( $p/s$ )	$p$ ( $p$ )	$s$ ( $s$ )	$p$ ( $s$ )	$p$ ( $p$ )
On/Off-Shell	Off	Off	On	On	On	On
DM Mass [GeV]	$\approx 40$	$\approx 40$	$\approx 80$	$\approx 80$	$\approx 120$	$\approx 120$

Table 2: Annihilation to mediators. S,P,V,A correspond to scalar, pseudoscalar, vector, and axial vector interactions with DM. Also shown: the leading velocity (partial wave) dependence, whether the process may occur on-shell, and the approximate mass for 40 GeV final state  $b$  quarks. The off-shell axial coupling is  $s$ - or  $p$ -wave for axial/vectorlike SM coupling respectively [120].

in the language of (2.1), whether or not the DM interactions are chiral. On the other hand, electroweak gauge invariance mandates chiral interactions for the mediator's SM coupling.

We are thus led to consider a hybrid description where the mediator's interaction with the SM is naturally described by a chiral coupling while the interaction with DM is most usefully described by a coupling of definite parity. The chiral description of the SM breaks down for direct detection; however, since chiral interactions generically include both the  $\mathbb{1}$  and  $\gamma^5$  terms, we focus on bounds from the parity-even interaction that yields stronger bounds. Dark matter searches at colliders probe relativistic energies without polarization information and are thus typically independent of parity. In this document we refer to the 'spin-0' or 'pseudoscalar' mediator to mean the spin-0 field which has a pseudoscalar interaction with the Dirac DM without assuming a particular parity-basis interaction to the SM.

## 2.2 Mediators Versus $s$ -wave Annihilation

The parity basis for dark matter interactions clarifies the types of interactions that can yield  $s$ -wave annihilation for the  $\gamma$ -ray excess. In Table 2 we show annihilation modes to up to three spin-0 or spin-1 mediators for the interactions in (2.1). On-shell kinematics require at least two final states so that the leading annihilation modes in the on-shell mediator limit are two spin-1 particles (of either parity) or three pseudoscalars. The off-shell diagrams represent the  $s$ -channel simplified models in [113, 114].

Also shown in Table 2 are the approximate masses for the on-shell mediator scenarios. In order to eject 40 GeV  $b$  quarks from each annihilation, the two (three) body final states require that the DM mass is approximately  $m_\chi = 80$  (120) GeV. Observe that this mechanism allows one to circumvent the conventional wisdom that the galactic center signal requires DM lighter than typical electroweak scale states.

Note that these masses are back-of-the-envelope estimates that do not account for the boost in the  $b$  spectrum from the mediator momentum or the spread in mediator energies for the 3-body final state. Further, we assume only couplings to  $b$ . This is a reasonable estimate and does not violate flavor bounds for spin-0 mediators since it follows approximately from minimal flavor violation (MFV) [121–124]. On the other hand, spin-1 mediators generically couple democratically to all three generations in the MFV ansatz, as can be seen when comparing (2.2) and (2.3). Finally, one should also account for the effect of the off-shell,  $s$ -channel annihilation modes for finite coupling

to the SM,  $\lambda_{\text{SM}}$ . We account for these in Sec. 3 where we perform a fit to the  $\gamma$ -ray excess.

The amplitudes for annihilation to two spin-1 mediators via the vector and axial interactions are identical so in this case the choice of parity versus chirality basis is irrelevant. Of the spin-0 mediators, however, only pseudoscalars generate  $s$ -wave annihilation. If the dark sector is described by a chiral theory, one generically expects both parities to be present. However, since the scalar is  $p$ -wave, it is suppressed by  $\langle v^2 \rangle \sim 10^{-6}$  and may be ignored for annihilation. On the other hand, this dramatically affects the direct detection rate, as discussed in Sec. 4.2.

## 2.3 Requirements for On-Shell Mediators

On-shell mediator models must satisfy the following conditions for the dark sector spectrum,

$$2m_\chi > \begin{cases} 2m_V & \text{for a spin-1 mediator} \\ 3m_\varphi & \text{for a spin-0 mediator} \end{cases} \quad (2.4a)$$

$$m_{V,\varphi} > 2m_b \quad (2.4b)$$

and the following requirements on the mediator couplings,

$$\lambda_{\text{DM}} \sim 1 \quad (2.4c)$$

$$\lambda_{\text{SM}} \ll 1. \quad (2.4d)$$

These are interpreted as follows:

- (a) Nonrelativistic DM annihilation has enough energy to produce on-shell mediators.
- (b) The mediator may decay into  $b$  quarks to produce the spectrum of the  $\gamma$ -ray excess.
- (c) The additional coupling(s) in the on-shell diagrams do not suppress the amplitude nor are they so large that they are nonperturbative,  $\lambda_{\text{DM}}^2 < 4\pi$ .
- (d) Parametrically suppress the off-shell,  $s$ -channel mediator diagrams in annihilation and simultaneously ameliorate limits from direct detection and colliders.

We now elucidate the conditions (2.4c–2.4d) more carefully by determining the coupling scaling of the on-shell versus off-shell annihilations. For a spin-1 mediator, the on-shell annihilation mode goes through two on-shell mediators which subsequently decay into  $b\bar{b}$  pairs. The key observation is that unlike the case of an off-shell  $s$ -channel mediator, the annihilation to on-shell mediators is largely independent of the coupling to the SM,  $\lambda_{\text{SM}}$ . We thus focus on the limit where the on-shell mode dominates over the off-shell  $s$ -channel diagram,

$$\left( \begin{array}{c} \chi \\ \chi \end{array} \right) \sim \lambda_{\text{DM}}^2 \gg \left( \begin{array}{c} \chi \\ \chi \end{array} \right) \sim \lambda_{\text{DM}} \lambda_{\text{SM}}. \quad (2.5)$$

Note that this condition is trivial if the mediator has axial couplings since the  $s$ -channel diagram is  $p$ -wave. As discussed above, in a UV model that avoids flavor bounds, a spin-1 mediator is likely to couple democratically to other SM fermion generations. The annihilation rate relevant to

the galactic center  $\gamma$ -ray excess would be multiplied by the branching ratio to  $b\bar{b}$  pairs,  $\text{Br}(V \rightarrow b\bar{b})$ . If one insists that the  $\gamma$ -ray excess is generated exclusively by the decay of  $b$  quarks, then the branching ratio is an additional  $\mathcal{O}(10^{-1})$  factor that must be compensated by  $\lambda_{\text{DM}}$ . More dangerously, one must also account for the  $\gamma$ -ray pollution from annihilations yielding light quarks. We address the effect of this pollution on the fit to the  $\gamma$ -ray spectrum in Sec. 6.1.

For a pseudoscalar mediator the analogous limit is

$$\left( \begin{array}{c} \chi \\ \chi \end{array} \rightarrow \begin{array}{c} \text{on shell} \end{array} \rightarrow \begin{array}{c} \text{three-body} \end{array} \right) \sim \frac{\lambda_{\text{DM}}^3}{\sqrt{4\pi}} \gg \left( \begin{array}{c} \chi \\ \chi \end{array} \rightarrow \text{two-body} \right) \sim \lambda_{\text{DM}} \lambda_{\text{SM}}. \quad (2.6)$$

We have also inserted an explicit factor of  $\sqrt{4\pi}$  for the additional phase space suppression in the cross section of a three- versus two-body final state.

Both (2.5) and (2.6) impose the limit  $\lambda_{\text{SM}} \ll 1$  to suppress the  $s$ -channel off-shell mediator with  $\lambda_{\text{DM}}$  fixed (for given masses) to give the correct galactic center photon yield. The magnitude of ‘ $\gg$ ’ is addressed in Sec. 4. The limit of a very small coupling to the Standard Model is further motivated by the dearth of observational evidence for dark matter interactions at colliders and direct detection experiments. This limit also occurs naturally in models of dark photon kinetic mixing or compositeness. In our scenario, parametrically suppressing this coupling increases the lifetime of the mediator. This has little phenomenological consequence given the astronomical distance scales associated with the galactic center.

## 2.4 Estimates for the $\gamma$ -ray Excess

Before doing a fit to the  $\gamma$ -ray excess, we establish a back-of-the-envelope benchmark using the DM masses in Table 2 and neglecting the mediator spectrum and boost. This gives a reasonable estimate while also highlighting the parametric behavior of the fit. The contact interaction fits to the galactic center  $\gamma$ -ray excess suggest annihilation to a pair of  $b$  quarks with a thermally averaged cross section [13],

$$\langle \sigma v \rangle_{b\bar{b}} \approx 5 \times 10^{-26} \text{ cm}^3/\text{s}. \quad (2.7)$$

Note that [14] found a slightly smaller cross section,  $1.5 \times 10^{-26} \text{ cm}^3/\text{s}$  due to a slightly tighter DM halo (larger  $\gamma$  parameter in the generalized NFW profile [125–127]). The photon spectrum from this annihilation is

$$\frac{d\Phi(b, \ell)}{dE_\gamma} = \frac{\langle \sigma v \rangle_{b\bar{b}}}{2} \frac{1}{4\pi m_\chi^2} \frac{dN_\gamma}{dE_\gamma} \int_{\text{LOS}} dx \rho^2(r_{\text{gal}}(b, \ell, x)), \quad (2.8)$$

where  $(b, \ell)$  are Galactic coordinates,  $\rho$  is the DM profile, and  $r_{\text{gal}}$  is the distance from the galactic center along the line of sight (LOS).

In on-shell mediator models, the DM annihilates into 2 (3) mediators which each decay into pairs of  $b$  quarks. In order that each of these final state  $b$  quarks to carry 40 GeV, the DM mass must be approximately 80 (120) GeV as stated in Table 2. This reduces the DM number density by 4 (9) in order to maintain the observed mass density; this is manifested in the  $m_\chi^{-2}$  factor



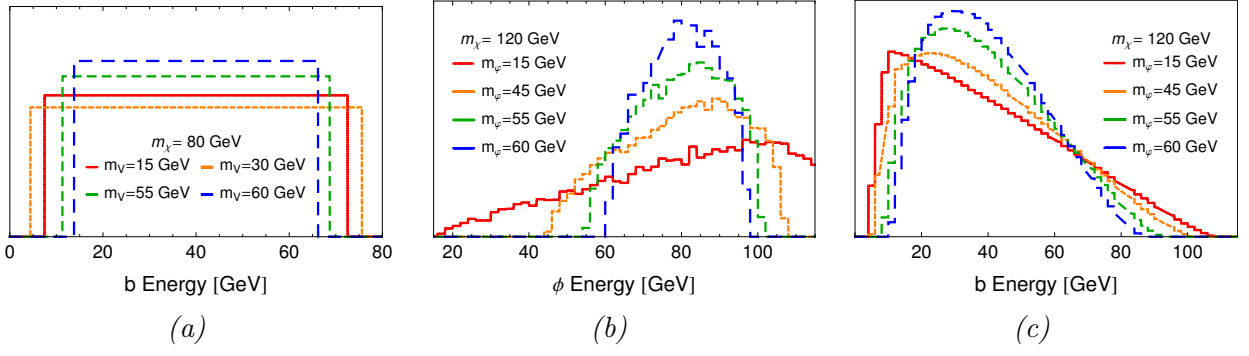


Figure 4: (a)  $\chi\bar{\chi} \rightarrow VV \rightarrow 4b$ , (b)  $\chi\bar{\chi} \rightarrow 3\phi$ , (c)  $\chi\bar{\chi} \rightarrow 3\phi \rightarrow 6b$ . Energy spectrum with arbitrary normalization from DM annihilation for (a)  $b$  quarks from two on-shell spin-1 mediators, (b) pseudoscalar mediators, (c)  $b$  quarks from three on-shell pseudoscalar mediators. (a) corresponds to  $m_\chi = 80$  GeV while (b,c) corresponds to  $m_\chi = 120$ . Lines correspond to  $m_V = 15, 30, 55, 60$  GeV or  $m_\phi = 15, 45, 55, 60$  GeV from red (solid) to blue (most dashed). The ‘box’ width in (a) is not monotonically decreasing with  $m_V$ , as evidenced by the 30 GeV line (orange).

of (2.8). This factor is partially compensated by the multiplicity of  $b\bar{b}$  pairs in the final state increases the total secondary photon flux by a factor of 2 (3). Together, these effects require that the annihilation cross section is a factor of  $\approx 2$  (3) times larger than  $\chi\bar{\chi} \rightarrow b\bar{b}$  cross section (2.7),

$$\langle\sigma v\rangle_{\text{ann.}} \approx 2(3) \times \langle\sigma v\rangle_{b\bar{b}}. \quad (2.9)$$

where  $\langle\sigma v\rangle_{b\bar{b}}$  is the contact interaction value (2.7). Because  $\langle\sigma v\rangle_{b\bar{b}}$  is already determined to be close to the thermal relic, one may worry if the additional factor in (2.9) violates the feasibility of a thermal relic. We address this in Sec. 5. Considering the range of kinematically allowed mediator masses and accounting for the powers of  $\lambda_{\text{DM}}$  in the spin-0 and spin-1 cases, (2.9) gives the estimate

$$\lambda_{\text{DM}} \sim 1.1 - 1.4 \quad (\text{spin-0}) \quad (2.10)$$

$$\lambda_{\text{DM}} \sim 0.27 - 0.44. \quad (\text{spin-1}) \quad (2.11)$$

These couplings indeed agree with the estimate (2.4c) while remaining perturbative,  $\lambda_{\text{DM}}^2 < 4\pi$ . The scale of the spin-1 coupling implies a slight suppression on the left-hand side of (2.5) which must be compensated by a stronger upper bound on  $\lambda_{\text{SM}}$ . We show below that direct detection also constraints  $\lambda_{\text{SM}}$  strongly for the spin-1 mediator.

### 3 The $\gamma$ -Ray Excess from On-Shell Mediators

Having established the intuition developed in Sec. 2.4, we examine the photon spectrum predicted from the on-shell mediator scenario and fit to the observed  $\gamma$ -ray excess.

#### 3.1 Mediator Spectra

In 2-to-2 scattering, the final state energies is completely determined by kinematics. This is the case for  $\chi\bar{\chi} \rightarrow b\bar{b}$  from effective contact interactions or simplified models with single off-shell mediators; the monochromatic spectrum of final state  $b$  quarks yield, upon showering, a spectrum of photons

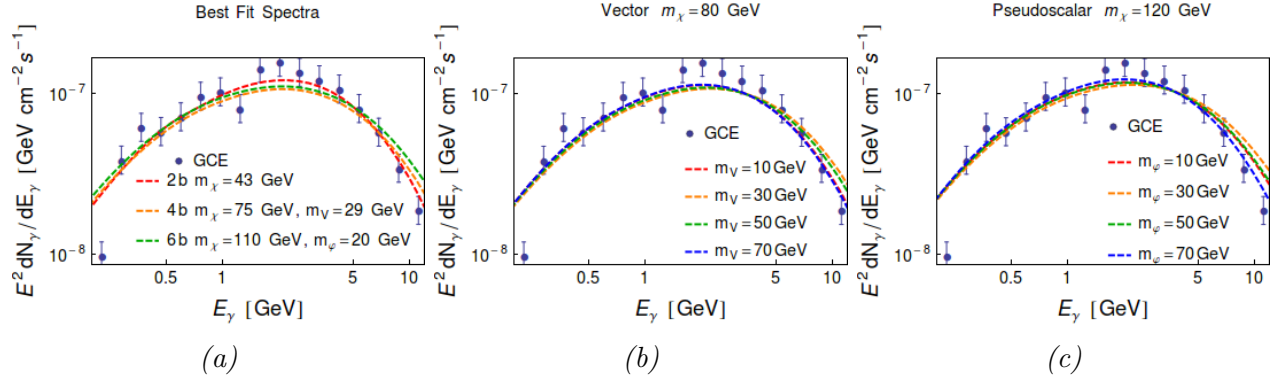


Figure 5: (a) Comparison, (b) Spin-1, (c) Spin-0. Predicted spectra for the galactic center  $\gamma$ -ray excess (GCE) for (a) the best fit models categorized by the number of final state  $b$  quarks, (b) a range of spin-1 mediator masses, (c) a range of spin-0 mediator masses. Overlaid is the measured  $\gamma$ -ray spectrum from [13], bars demonstrate an arbitrary measure of goodness-of-fit. See Sec. 3.3 for details.

which fits the observed  $\gamma$ -ray excess well. In the case of annihilation to on-shell mediators, however, the  $b$  quark spectrum is no longer monochromatic, as shown in Figure 4.

For spin-1 mediators, it is well known that the final states of a  $\chi\bar{\chi} \rightarrow VV \rightarrow 4b$  cascade has box-like energy spectrum over the kinematically allowed range; see, for example, [128, 129]. The  $V$  spectrum is monochromatic in the lab frame and the  $b\bar{b}$  spectrum is monochromatic in the  $V$  rest frame. The  $b$  energies in the lab frame depend on the angle of the  $b\bar{b}$  axis relative to the direction of the  $V$  boost. Isotropy of the  $V$  boost washes out the angular dependence and gives a flat  $b$  spectrum over the kinematically allowed region. This is demonstrated in Fig. 4(a). The box becomes more sharply peaked as  $m_V \rightarrow m_\chi = 40$  GeV. The case of annihilation into three spin-0 mediators is more complicated since the mediators have a nontrivial energy spectrum and it is no longer simple to derive the  $b$  spectrum from kinematics alone. Monte Carlo energy spectra for  $\chi\bar{\chi} \rightarrow 3\phi$  and the subsequent decay in to  $6b$  are shown in Fig. 4(b,c) using MadGraph 5 [130].

### 3.2 Generating $\gamma$ -Ray Spectra

$\gamma$ -ray spectra for our simplified models are generated using PPC 4 DM ID (henceforth PPC) [131–133], a *Mathematica* [134] package that generates indirect detection spectra based on data extracted from PYTHIA 8 [135]. Presently, PPC only generates signals for DM annihilation into pairs of SM particles. In order to include the effects of the on-shell mediators, one must account for the boost by convolving the PPC photon spectrum  $dN_\gamma(E_b)/dE_\gamma$  with a distribution of  $b$  energies  $E_b$  which may be taken as a box for the case of two on-shell mediators or interpolated from Monte Carlo simulations such as Fig. 4(c).

For on-shell annihilation into spin-0 and spin-1 mediators, the shape of the photon spectrum is completely determined by the masses of the DM particle  $m_\chi$  and the mediator  $m_{\phi,V}$  while the overall normalization is fit to the necessary cross section by fixing  $\lambda_{\text{DM}}$ , as estimated in (2.10 – 2.11). The effect of the mediator mass is fairly modest, as demonstrated in the  $E_\gamma^2 dN_\gamma/dE_\gamma$  spectra in Fig. 5. The reason for this is that the requirement that the mediator is massive enough to decay into  $b\bar{b}$  pairs (2.4d) limits the extent to which the mediators are boosted.

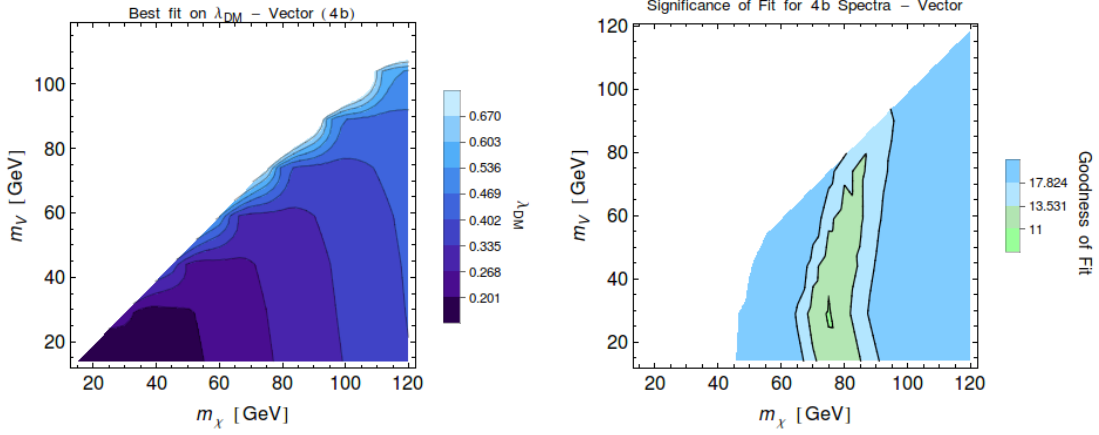


Figure 6: Fits for on-shell annihilation through spin-1 mediators. LEFT: best fit values of  $\lambda_{\text{DM}}$ . RIGHT: fit significance highlighting the best  $(m_\chi, m_{\text{med.}})$  values. See text for details.

### 3.3 Fitting the $\gamma$ -Ray Excess

We use the  $\chi\bar{\chi} \rightarrow b\bar{b}$   $\gamma$ -ray excess spectrum assuming a  $\chi\bar{\chi} \rightarrow b\bar{b}$  template from Figure 8 of [13]. We note, however, that this is an approximation since the on-shell mediator scenario predicts a different spectral shape that, in principle, should be modeled and included in the fit for the  $\gamma$ -ray excess. The comparison of the best fit  $\chi\bar{\chi} \rightarrow 2b$  spectrum versus the on-shell mediator spectra in Fig. 5(a) qualitatively demonstrates the degree of approximation.

Indeed, [13] showed how the spectrum of the excess (though not its existence) can depend on both the background subtraction and the choice of DM template assumed in the fit. This highlights a second caveat when building DM models for the  $\gamma$ -ray excess. As is standard in astrophysics literature, [13] and [14] only quote statistical errors on their fits since the systematic errors associated with fitting and subtracting background is nontrivial and intractable to quantify. Both [13] and [14] make this clear in their text. Model builders from the particle physics community, however, should be careful not to interpret these statistical uncertainties in the same way as quoted uncertainties from collider data, where both statistical and systematic errors are included. [13] demonstrated some of the systematic uncertainties by exploring the differences in the spectral fits from different background subtraction. Further still, both [13] and [14] use the FERMI collaboration's 2FGL point sources and recommended diffuse emission model `gal_2yearp7v6_v0`. These assumptions also carry an implicit systematic uncertainty that are difficult to quantify without further input from the FERMI collaboration.

That being said, one can see from the  $1\sigma_{\text{stat.}}$  error bars in Fig. 5 of [14] that even just the statistical errors on the  $\gamma$ -ray excess can accommodate modified spectra. Combined with the estimated systematic errors in Figure 8 of [13] and additional systematic errors from the FERMI background, this suggests that more general final states beyond the standard  $b\bar{b}$  and  $\tau\bar{\tau}$  should be considered for the  $\gamma$ -ray excess. In Appendix A we present simple explorations for the range of spectra that can be generated in the on-shell mediator scenario.

Because of the unquantified systematic error associated with these spectra, we do not parameterize the statistical significance of our fits in terms of confidence intervals. Instead, we measure the goodness of fit using the  $\chi^2$  value with an arbitrarily chosen 20% error,

$$\text{goodness of fit} = \sum_i \left( \frac{\log D_i - \log(\lambda_{\text{DM}}^{2n} S_i)}{\log(0.2D_i)} \right)^2. \quad (3.1)$$

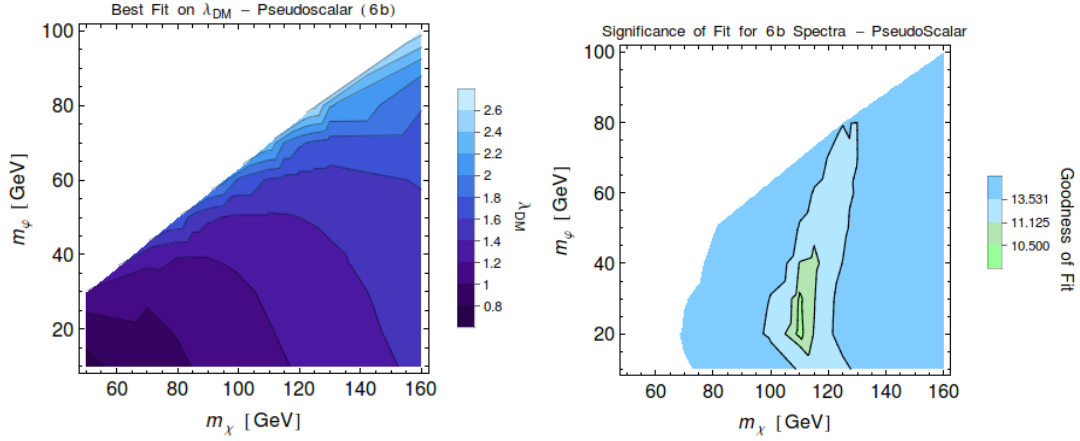


Figure 7: Fits for on-shell annihilation through spin-0 mediators. LEFT: best fit values of  $\lambda_{\text{DM}}$ . RIGHT: fit significance highlighting the best  $(m_\chi, m_{\text{med.}})$  values. See text for details.

Smaller values are better fits. The index  $i$  runs over the bins in the extended source data set,  $D$  and  $S$  are the  $E_\gamma^2 \frac{dN_\gamma}{dE_\gamma}$  values for the extended source data and the model spectra (assuming  $\lambda_{\text{DM}} = 1$ ) respectively, and  $\lambda_{\text{DM}}^{2n}$  is the overall normalization of our input spectra, where  $n = 2, 3$  is the number of on-shell mediators produced in each annihilation. The denominator reflects the assumed 20% error: we emphasize that this is not a statement about the total error, but rather a standard candle for quantifying the goodness-of-fit. This is shown as a bar on the data in Fig. 5.

In Figs. 6 and 7 we fit the spectral shape over the region of DM and mediator masses,  $m_\chi$  and  $m_{\text{med.}}$ , estimated in Table 2 and (2.4a – 2.4b). The DM coupling  $\lambda_{\text{DM}}$  parameterizes the overall normalization and is fixed to minimize (3.1) for each value of  $m_\chi$  and  $m_{\text{med.}}$ . The best fit values prefer a slightly lighter DM particle than the back-of-the envelope estimates in Table 2 due to the on-shell mediator smearing the  $b$  spectrum. The fits are flexible over the range of mediator masses within the kinematically accessible region, as seen in Fig. 5(b,c). We note that these plots assume the limit of vanishing SM coupling,  $\lambda_{\text{SM}} \rightarrow 0$ , so that the contribution to the  $\gamma$ -ray spectrum from  $\chi\bar{\chi} \rightarrow b\bar{b}$  via  $s$ -channel, off-shell mediators is negligible. We explore the role of finite  $\lambda_{\text{SM}}$  in Sec. 4.1. We also note that the simplest models spin-1 mediators typically have universal couplings to all quark generations; we address this in Sec. 6.1 and display the modified results in Fig. 10.

## 4 Experimental Bounds on the SM Coupling

One of the features of the on-shell mediator scenario is that the  $\gamma$ -ray excess annihilation mode is controlled by parameters that can be independent of the conventional experimental probes for DM–SM interactions. Following the complementarity in Fig. 2, we examine the effect of non-negligible mediator coupling to the SM and determine the bounds on  $\lambda_{\text{SM}}$ .

In contrast to effective contact interactions or models with off-shell mediators, the on-shell mediator scenario naturally includes the limit of extremely small SM coupling so that it is always possible to parametrically ‘hide’ from these bounds. In principle, one may invoke the morphology of the  $\gamma$ -ray excess to set a lower bound on the mediator coupling. For example, if the mediator decay were too suppressed, the observed  $\gamma$ -ray excess would have a spatial extent larger than the galactic center. In fact, the DM interpretations in [7, 14] found that the excess has a tighter profile ( $\gamma > 1$ ) than the standard NFW DM density profile [125–127]. This lower bound on  $\lambda_{\text{SM}}$  is effectively irrelevant because of the astronomical distances associated with the galactic center.

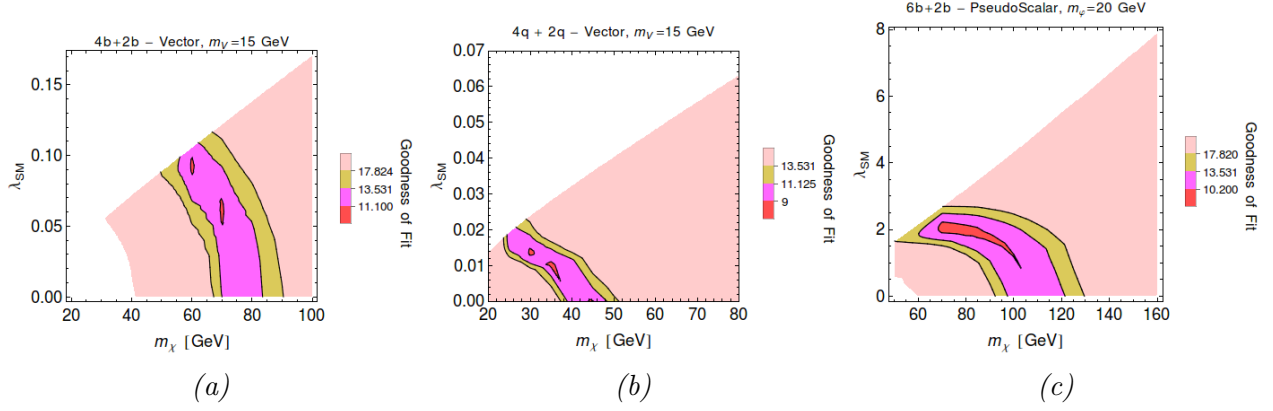


Figure 8: (a) *Spin-1 (b-philic)*, (b) *Spin-1 (q-democratic)*, (c) *Spin-0*. Fits including *s*-channel diagrams to the case of a (a) *spin-1* mediator coupling only to *b*, (b) *spin-1* mediator coupling to all quarks equally, and (c) *pseudoscalar* mediator. Plots assume that the *s*-channel diagrams are *s*-wave, see Tab. 2. Smaller values correspond to better fits, see (3.1).

## 4.1 Indirect Detection

In Sec. 3 we assumed that the contribution of *s*-channel diagrams to DM annihilation is negligible following (2.5 – 2.6). We can use the arbitrarily normalized goodness-of-fit measure (3.1) to assess the effect of these diagrams on the  $\gamma$ -ray excess fit as we parametrically increase  $\lambda_{\text{SM}}$ . We assume that the mediator couplings are such that the *s*-channel diagram supports *s*-wave annihilation, otherwise the contribution is negligible due to *p*-wave suppression by  $\langle v^2 \rangle \sim 10^{-6}$ . From Table 2, we see that non-negligible *s*-channel contributions may come from mediators with either pseudoscalar or vector coupling to the SM. For example, *V* could couple axially to both DM and the SM with a large *s*-channel contribution for finite  $\lambda_{\text{SM}}$ . On the other hand, if *V* couples axially to DM and vectorially to the SM, then there may be little modification to the annihilation spectrum from *s*-channel diagrams even for large values of  $\lambda_{\text{SM}}$ .

We scan over values of  $\lambda_{\text{SM}}$  that parametrically increases the relative fraction of *s*-channel off-shell DM annihilations to on-shell annihilations to mediators<sup>5</sup>, allowing  $\lambda_{\text{DM}}$  and the mediator mass to float to a best-fit value. The results of the fit are shown in Fig. 8, where the best fit regions have smeared into lower DM masses compared to Fig. 6. The *s*-channel contribution produces  $\gamma$ -ray spectrum which is a poor fit due to the larger DM mass in the on-shell mediator limit. However, because the  $\gamma$ -ray spectrum is smeared out relative to the *b* spectrum, there are intermediate masses  $m_\chi$  where the harder-than-usual *s*-channel diagram and the softer-than-usual on-shell mediator diagram average to yield good spectral fits. From the point of view of constructing DM models for the  $\gamma$ -ray excess, this shows that not only can the DM particle be as heavy as 80 or 120 GeV, as shown in Sec. 2, but it can take on intermediate values between these values and  $m_\chi \approx 40$  GeV. We further generalize this in Appendix A where we find plausible fits with  $m_\chi < 40$  GeV, and propose a simple mechanism to make  $m_\chi > 120$  GeV.

We note that in this scenario, indirect detection bounds from cosmic antiprotons can constrain  $\lambda_{\text{DM}}$ . Current constraints from the PAMELA are not sensitive to the rates required in our model, though AMS-02 will access this region [136, 137]<sup>6</sup>.

<sup>5</sup> Note from (2.5 – 2.6) that the relative ratio of *s*-channel diagrams to on-shell mediator diagrams is determined not simply by  $\lambda_{\text{SM}}$ , but a ratio of  $\lambda_{\text{SM}}$  to a power of  $\lambda_{\text{DM}}$  depending on the type of mediator.

<sup>6</sup>We thank KC Kong for pointing this out. See Fig. 2 and Fig. 4 of [136] for the relevant bounds, recalling (2.9)

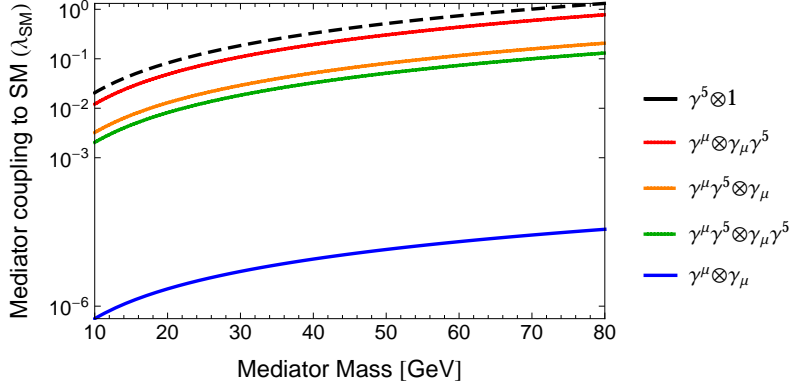


Figure 9: Estimated direct detection bounds on the mediator–SM coupling ( $\lambda_{\text{SM}}$ ) for interactions  $\mathcal{O}_\chi \otimes \mathcal{O}_q$  defined in (1.1). The dashed (solid) lines assume the benchmark value  $m_\chi = 120$  (80) GeV for spin-0 (1) mediators and the median DM couplings in (2.10–2.11).

## 4.2 Direct Detection

Unlike the other experimental options in Fig. 2, direct detection experiments probe WIMP–nucleon interactions at low transfer momentum,  $q^2 \sim \mathcal{O}(10 \text{ MeV})$ , and are accurately described in the contact interaction limit with corrections of order  $\mathcal{O}(q^2/m_{\text{med}}^2) \ll 1$ . The present experimental bounds on the spin-independent (SI) and spin-dependent (SD) interactions in the DM mass region of interest are set by the LUX [109] and XENON 100 [138] collaborations, respectively:

$$\sigma_{\text{SI}} \lesssim 10^{-45} \text{ cm}^2 \quad \sigma_{\text{SD}} \lesssim 5 \times 10^{-40} \text{ cm}^2. \quad (4.1)$$

In Fig. 9 we apply these bounds to the contact interactions in (1.1) with the identification  $\Lambda^{-2} = \lambda_{\text{SM}} \lambda_{\text{DM}} / m_{\text{med}}^2$ . We use the benchmark parameters in Section 2.4 with the fact that the spin-0 mediator couple only to  $b$  quarks while the spin-1 mediator couples universally to all quarks.

In addition to the conventional spin-independent ( $\gamma^\mu \otimes \gamma_\mu$ ) and spin-dependent ( $\gamma^\mu \gamma^5 \otimes \gamma_\mu \gamma^5$ ) interactions, we present bounds on the axial–vector ( $\gamma^\mu \gamma^5 \otimes \gamma_\mu$ ) and vector–axial ( $\gamma^\mu \otimes \gamma_\mu \gamma^5$ ) interactions for a spin-1 mediator. These are suppressed by virtue of being higher order in the transfer momentum/DM velocity; we estimate these bounds following [66]. If the spin-1 mediator couples only to  $b$  quarks, the bound on  $\lambda_{\text{SM}}$  is weakened because interactions with target nucleons go through a  $b$ -quark loop that induces mixing between the mediator and the photon [114, 139].

As discussed in Sections 2.1 and 2.2, we only consider spin-0 mediators that couple as a pseudoscalar to DM. We do not include the  $\gamma^5 \otimes \gamma^5$  operator since it is so suppressed by powers of the momentum transfer that the bounds on  $\lambda_{\text{SM}}$  are weaker than the perturbativity bound  $\lambda_{\text{SM}} < \sqrt{4\pi}$ . We evaluate momentum-dependent operators at  $q^2 = 0.1 \text{ GeV}$  following [66]. These direct detection rates can be calculated in more detail using the nonrelativistic effective theory developed in [63, 65, 69]. Operator bounds in this formalism are presented in [140, 141] and *Mathematica* codes for these calculations are available in [141] and [64].

## 4.3 Collider bounds

The collider bounds for this class of models falls into two types: those based on processes where the mediator couples to both the SM and DM and those that only depend on the mediator’s coupling to the SM.

---

for our model. Note, however the large propagation uncertainties in Fig. 2.



The first type of collider bounds are epitomized by mono-object searchers with missing energy where the DM leaves the collider. These bounds are discussed extensively in the  $\gamma$ -ray [off-shell,  $s$ -channel] simplified models [14, 114]. We thus only highlight the most promising proposed bound, the ‘mono- $b$ ’ search [50]. Because of the requirement (2.4c) of on-shell annihilation into mediators, the class of models explored in this paper typically falls in the range where the effective contact interaction description breaks down [35, 72–75]. We leave a detailed simplified model study for future work, but instead translate the projected scalar–scalar ( $\mathbb{1} \otimes \mathbb{1}$ ) contact interaction bounds in [50] as a conservative estimate for the reach of this search. Over the range of dark matter masses  $m_\chi \lesssim 150$  GeV, the projected bound from 8 TeV LHC data is approximately

$$M_* > 100 \text{ GeV} \quad \Rightarrow \quad \lambda_{\text{SM}}^{\text{spin-0}} \lesssim 0.2, \quad \lambda_{\text{SM}}^{\text{spin-1}} \lesssim 0.6, \quad (4.2)$$

where  $M_*$  parameterizes the scalar–scalar contact interaction,

$$\frac{m_q}{M_*^3} (\bar{\chi}\chi) (\bar{q}q). \quad (4.3)$$

To estimate this bound, we have matched this to  $\lambda_{\text{SM}} \lambda_{\text{DM}} s^{-1} (\bar{\chi}\chi) (\bar{q}q)$ , where we have taken  $s = 225$  GeV, the cut on the minimum missing energy in [50]. We have estimated that the spin-1 bound on  $M_*$  is identical and used the smaller  $\lambda_{\text{DM}}$  value (2.11). Note that at high energies the distinction between operators with and without a  $\gamma^5$  in the parity basis is negligible. The bound (4.2) is thus fairly robust; unlike the direct detection bounds, a judicious choice of operator cannot avoid the constraints from this search.

A second class of collider bound comes from a search for the signatures of the mediator interacting only with the SM sector. The bounds from this type of search are relatively weak in the mediator mass range of interest (15 – 70 GeV) because of large QCD backgrounds in bump searches (dijet,  $4b$ ); see, for example, [142]. Because our only requirement is that the mediator couple to  $b$  quarks (and other quarks as mandated by MFV, for example), a prototype for the mediator is a  $Z'$  that gauges baryon number  $U(1)_B$ . This has been examined originally in [143, 144] where the most stringent bounds come from the hadronic width of the  $Z$  which sets a relatively weak bound

$$\lambda_{\text{SM}} \lesssim 1. \quad (4.4)$$

This bound becomes stronger in the neighborhood of the  $\Upsilon$  mass, but this is already at the edge of what is kinematically allowed for decay into  $b$  pairs (2.4d). See also [145] for a review including loop-level constraints from mixing and [146] for discussion of bounds combined with anomaly constraints. Another prototype for the spin-0 mediator is a gauge-phobic, leptophobic Higgs. There exist very few bounds for such an object in the mass range of interest. A preliminary estimate for the reach of a ‘Higgs’ diphoton search between 50 – 80 GeV ATLAS detector with 20/fb found weaker constraints than (4.4) [147].

## 5 Viability as a Thermal Relic

One of the appealing features of the simplest  $\chi\bar{\chi} \rightarrow b\bar{b}$  mode is that the required annihilation cross section (2.7) is so close to the value required for a thermal relic. Due to the scaling in (2.8), the  $s$ -wave annihilation cross section for the on-shell mediator scenario is a factor of  $n$  larger than the thermal value where  $n = 2, 3$  is the number of mediators emitted, (2.9). This comes from a factor of  $n$  enhancement due to the number of  $b\bar{b}$  final states and a factor of  $n^2$  suppression coming from

a decreased DM number density. We examine the extent to which our scenario may still furnish a standard thermal relic. Observe that this sector of the model no longer has free parameters since the  $\gamma$ -ray excess fixes both the dark matter mass  $m_\chi$  and coupling  $\lambda_{\text{DM}}$ .

## 5.1 $s$ -wave Cross Section

For simplicity, let us first assume that DM annihilation at freeze-out is dominated by the same diagrams that generate the galactic center  $\gamma$ -ray excess at the present time. We address  $s$ -channel and  $p$ -wave corrections below. The observed Dirac DM density  $\Omega_\chi h^2$  is approximately<sup>7</sup> [149]

$$\Omega_\chi h^2 \approx \frac{6 \times 10^{-27} \text{ cm}^3/\text{s}}{\langle \sigma v \rangle_{\text{ann.}}} \quad (\Omega_\chi h^2)_{\text{obs.}} = 0.12 \quad [150\text{--}152] \quad (5.1)$$

where  $h$  is the Hubble constant in units of  $100 \text{ km}/(\text{s} \cdot \text{Mpc})$ . From (2.9), the annihilation cross section is  $\langle \sigma v \rangle_{\text{ann.}} \approx n(5 \times 10^{-26} \text{ cm}^3/\text{s})$ , where  $n = 2$  or  $3$  depending on the mediator. At face value, this gives a relic abundance that is too small. One may not mitigate this by assuming another DM component since this, in turn, reduces the galactic center signal and hence requires one to increase the annihilation cross section further.

While the value of  $\Omega_\chi h^2$  is well measured, the precise value of the annihilation cross section  $\langle \sigma v \rangle_{\text{ann.}}$  at freeze-out carries uncertainties from early universe parameters such as the number of effective degrees of freedom. On top of this, there are further uncertainties in our approximation (2.9) coming from uncertainties in astrophysical parameters. For example, the  $\chi\bar{\chi} \rightarrow b\bar{b}$  annihilation cross section (2.7) depends on the fit to the dark matter density profile at the center of the galaxy [153]. The analysis in [14] found a tighter density profile for which  $\langle \sigma v \rangle_{b\bar{b}} \approx 1.5 \times 10^{-26} \text{ cm}^3/\text{s}$ . The value of  $\langle \sigma v \rangle_{\text{ann.}}$  spin-1 mediators ( $n = 2$ ) required for a thermal relic falls between these two estimates of  $\langle \sigma v \rangle_{b\bar{b}}$ . We may thus assume that it is consistent with the galactic center signal within the uncertainty of the DM morphology. In fact, when the boost from the on-shell mediator is taken into account, the best fit DM mass is slightly smaller than the assumed 80 GeV in our estimate. This can push the estimated relic abundance from  $\Omega_\chi h^2 = 0.10$  to 0.12 so that the case of a spin-1 mediator may plausibly yield the correct thermal relic abundance. On the other hand, it is difficult for a spin-0 mediator to satisfy the observed DM relic abundance and seems to require additional mechanisms to produce  $\Omega_\chi h^2$ .

## 5.2 $s$ -channel and $p$ -wave Corrections

The corrections to the above estimates include  $s$ -channel  $\chi\bar{\chi} \rightarrow b\bar{b}$  diagrams and  $p$ -wave corrections from additional on-shell mediator diagrams. The  $s$ -channel modes are parametrically suppressed by  $\lambda_{\text{SM}}^2 \ll 1$  in the cross section and can be ignored.

Corrections from  $p$ -wave diagrams are negligible for present day annihilation in the galactic center due to a large velocity suppression. At the time of DM freeze-out, on the other hand, this velocity suppression is much weaker and one should check for  $p$ -wave corrections to the relic abundance. For spin-1 mediators there are no additional diagrams which are not suppressed relative to the  $\chi\bar{\chi} \rightarrow VV$   $s$ -wave diagram. For pseudoscalars mediators, on the other hand, the  $\chi\bar{\chi} \rightarrow 2\varphi$  mode is  $p$ -wave but not parametrically suppressed by  $\lambda_{\text{SM}}$ . At freeze-out these diagrams

---

<sup>7</sup>The thermal cross section for Dirac DM is a factor of 2 larger than Majorana DM [148].



may contribute appreciably to DM annihilation,

$$\left( \begin{array}{c} \chi \\ \chi \end{array} \right) \begin{array}{c} \nearrow \\ \searrow \\ \nearrow \\ \searrow \end{array} \begin{array}{c} \text{---} \\ \text{---} \\ \text{---} \\ \text{---} \end{array} \begin{array}{c} \nwarrow \\ \swarrow \\ \nwarrow \\ \swarrow \end{array} \left( \begin{array}{c} \chi \\ \chi \end{array} \right) \sim \frac{\lambda_{\text{DM}}}{\sqrt{4\pi}} \sqrt{\frac{x_f}{3}} \left( \begin{array}{c} \chi \\ \chi \end{array} \right) \begin{array}{c} \nearrow \\ \searrow \\ \nearrow \\ \searrow \end{array} \begin{array}{c} \text{---} \\ \text{---} \\ \text{---} \\ \text{---} \end{array} \begin{array}{c} \nwarrow \\ \swarrow \\ \nwarrow \\ \swarrow \end{array} \left( \begin{array}{c} \chi \\ \chi \end{array} \right) \quad (5.2)$$

on shell

The prefactor accounts for the additional phase space and  $p$ -wave suppression. The ratio of the DM mass to the freeze-out temperature  $x_f = m_\chi/T_f \approx 20$  appears when thermally averaging the annihilation cross section at freeze-out over a Maxwell–Boltzmann velocity distribution. This factor is not especially large and so one expects the pseudoscalar annihilation cross section at freeze-out to be even larger than approximated with only the  $s$ -wave piece. This further reinforces the observation that this class of mediator requires additional mechanisms to attain the observed DM relic density. See [154–172] for a partial list of model-building tools for obtaining the correct relic abundance without the standard freeze-out mechanism.

### 5.3 MSPs Can Save Freeze-Out

As noted in the Introduction, [7, 8, 11, 13, 26, 173] have pointed out that an alternate source for the  $\gamma$ -ray excess is a population of hitherto unobserved millisecond pulsars (MSPs). As an estimate, a few thousand MSPs could generate the observed  $\gamma$ -ray flux [13]. A recent study of low-mass X-ray binaries (LMXB) may lend credence to this argument. It is thought that MSPs are old pulsars that have been spun up ‘reborn’ due to mass accretion from a binary companion and that LMXB are simply a different phase of the same binary system. During accretion, the system is X-ray luminous and is categorized as an LMXB. The X-ray flux drops when the accretion rate drops and the system is then observed as a MSP. One can thus attempt to use the spatial distribution of the LMXB as a proxy for that of MSPs. [174] found that the spatial morphology of the LMXB in M31 is consistent with both the  $\gamma$ -ray excess and the DM interpretation—thus making it difficult to distinguish the two [27].

This, however, can be a boon for model-building within our DM framework. [7] noted that the degeneracy between the MSP and DM interpretations of the excess suggests that the excess may come from a combination of the two sources. In this way one may take the DM annihilation cross section to be that which is required for a thermal relic—thus undershooting the expected  $\gamma$ -ray flux—and then posit that a MSP population accounts for the remainder of the  $\gamma$ -ray excess.

### 5.4 Conditions for Thermal Equilibrium

In order for the thermal freeze-out calculation for  $\chi$  to be valid, we must assume that the mediator is in thermal equilibrium when the DM freezes out. This imposes a lower bound on the coupling of the mediator to the SM. In principle one must solve the Boltzmann equation for the mediator, but to good approximation it is sufficient to impose  $H \ll \Gamma(\text{med} \rightarrow b\bar{b})$ . For the range of mediators that can give the  $\gamma$ -ray excess, this imposes a very modest lower bound  $\lambda_{\text{SM}} \gtrsim 10^{-9}$ .

## 6 Comments on UV Completions and Model Building

Simplified models, such as those presented here, are bridges between experimental data and explicit UV models. In this section we highlight connections between our on-shell simplified models and viable UV completions.

### 6.1 Minimal Flavor Violation

The simplified models constructed in Section 2 couple the mediator only to  $b$  quarks to fit to the galactic center extended  $\gamma$ -ray source. Assuming only this coupling violates flavor symmetry and can lead to strong constraints from flavor-changing neutral currents. A standard approach to this issue in models of new physics is to impose the minimal flavor violation (MFV) ansatz where the Yukawa matrices are the only flavor spurions in the new physics sector [121–124]. This prescribes a set of relative couplings to the SM fermions up to overall prefactors. We assume that the dark sector is flavor neutral, see [24, 175, 176] for models with nontrivial flavor charge.

For the pseudoscalar mediator this is a small correction as can be seen by writing out the flavor indices in the spin-0 fermion bilinears (2.2) by which the pseudoscalar couples to the quarks. MFV mandates insertions of the Yukawa matrices between couplings of right- and left-handed fermions. After rotating to mass eigenstates this yields mediator–SM interactions

$$\mathcal{L}_{\varphi\text{-SM}} = \lambda_u \frac{m_{u_i}}{\Lambda} \varphi \bar{u}_{Li} u_{Ri} + \lambda_d \frac{m_{d_i}}{\Lambda} \varphi \bar{d}_{Li} d_{Ri} + \lambda_\ell \frac{m_{\ell_i}}{\Lambda} \varphi \bar{\ell}_{Li} \ell_{Ri}, \quad (6.1)$$

where  $q_{L,R} = P_{L,R}q$ , the  $\lambda_{u,d,\ell}$  are overall prefactors, and  $\Lambda$  is a UV flavor scale. Assuming that the  $\lambda_{u,d,\ell}$  are the same order naturally sets the dominant  $\varphi$  decay mode to be  $b\bar{b}$  since the  $t\bar{t}$  mode is kinematically inaccessible for the range of masses we consider. The simplified model coupling to  $b$  quarks is thus identified as

$$\lambda_{\text{SM}} = \lambda_d \frac{m_b}{\Lambda}. \quad (6.2)$$

The results of the simplified model above should be adjusted by including the effects of the other  $\varphi$  decay modes, though these effects are suppressed by the relative size of the other fermion masses to  $m_b$ . We remark that modest to large values of  $\lambda_u$  can lead to new signatures such as mediator emission off of a top quark at the LHC or gluon couplings through top loops.

The spin-1 mediators couple fermions of the same chirality, as demonstrated in (2.3). Promoting these interactions to an MFV-compliant coupling does not introduce additional factors of the Yukawa matrices since each term is a flavor singlet. Thus, unless the UV model is specifically constructed so that the spin-1 mediator couples preferentially to  $b$  quarks, the generic expectation is the spin-1 mediators have a universal coupling to each generation, for example

$$(\lambda_{\text{SM}})_d = (\lambda_{\text{SM}})_s = (\lambda_{\text{SM}})_b, \quad (6.3)$$

and similarly for the up-type quarks, leptons, and neutrinos. Unlike the case of the pseudoscalar mediator, this can lead to dramatic modifications since the light quarks produce a softer spectrum of secondary photons relative to the  $b$ . This is demonstrated in Fig. 10 which shows that the best fit spectrum is very different from that of the case where the spin-1 mediator only couples to the  $b$ : the best fit DM mass is  $\approx 45$  GeV rather than  $\approx 75$  GeV.

As a caveat, we note that for fitting the  $\gamma$ -ray excess with either spin-0 or spin-1 mediators, it is sufficient that  $\lambda_d$  is nonzero. Thus, in principle, one can set  $\lambda_u$  and  $\lambda_\ell$  to vanish; the latter condition suppresses the leptonic signals for the mediator at colliders and skirts the most stringent constraints on bosons in the on-shell mediator mass range (2.4a – 2.4b).

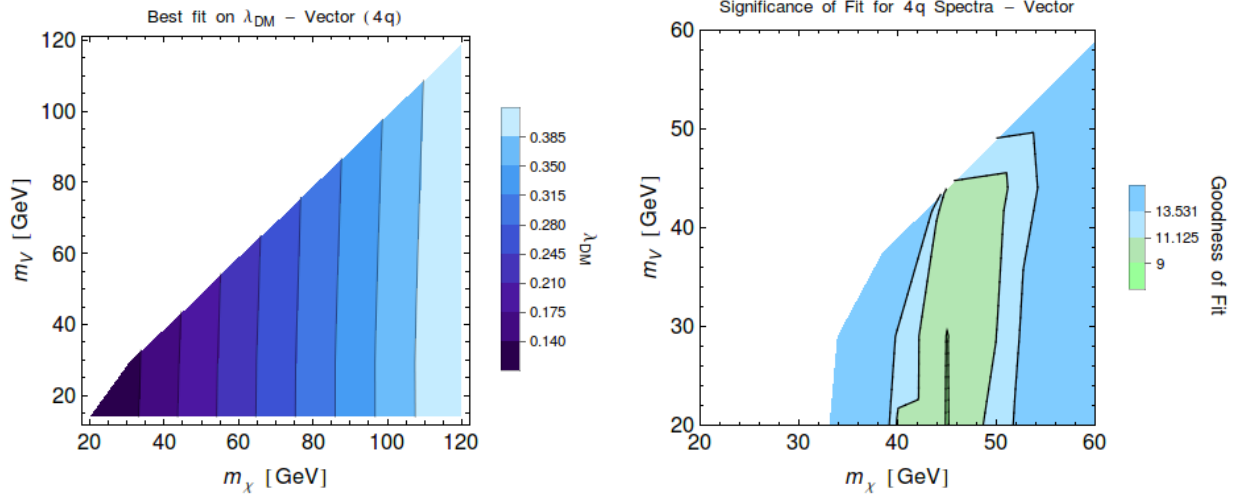


Figure 10: Fits for on-shell annihilation through spin-1 mediators assuming universal coupling to all quarks; compare to Fig. 6 which assumed a coupling to only  $b$  quarks. LEFT: best fit values of  $\lambda_{\text{DM}}$ . RIGHT: fit significance highlighting the best  $(m_\chi, m_{\text{med.}})$  values. See Section 3.3 for details.

## 6.2 Gauge symmetries

Gauge invariance also constrains UV completions of these simplified models. Because the SM fermions are chiral, the parity basis spin-0 interactions on the left-hand side of (2.2) are not  $\text{SU}(2)_L \times \text{U}(1)_Y$  gauge invariant. The similarity of (6.1) to the Yukawa coupling gives a hint for how to make this interaction SM gauge invariant. The  $m_b \bar{b}_R b_L$  term is implicitly  $y_b(v/\sqrt{2})\bar{b}_R b_L$ , where  $v$  is the Higgs vacuum expectation value. We may promote this to a gauge invariant coupling by restoring the Higgs doublet  $H$  so that (6.1) becomes

$$\mathcal{L}_{\varphi\text{-SM}} = \frac{\lambda_u y_{ij}^u}{\Lambda} \varphi H \cdot \bar{Q} u_R + \frac{\lambda_d y_{ij}^d}{\Lambda} \varphi \tilde{H} \cdot \bar{Q} d_R + \frac{\lambda_\ell y_{ij}^\ell}{\Lambda} \varphi \tilde{H} \cdot \bar{L} \ell_R, \quad (6.4)$$

where  $\tilde{H} = i\sigma^2 H^*$ ,  $Q$  and  $L$  are the left-handed  $\text{SU}(2)$  doublets.

UV models for the spin-1 mediators are also constrained by gauge invariance since these couplings can be assumed to be interactions of a spontaneously broken  $\text{U}(1)$  gauge symmetry. In a UV model one must be able to assign messenger charges to the SM fermions—or otherwise introduce new matter in the dark sector—to cancel all gauge anomalies with respect to the mediator gauge symmetry. The axial mediator case requires particular care since the global chiral symmetry of the SM is anomalous requiring, for example, a cancellation between the up-type and down-type quarks. See [146] for a recent analysis of anomaly constraints on the phenomenology of  $Z'$  bosons in the mass range and with the type of leptophobic/gauge-phobic couplings we consider for on-shell mediators for the  $\gamma$ -ray excess.

## 6.3 Renormalizability

Finally, one may push further and argue that a true ‘simplified model’ should depend only on renormalizable couplings; i.e. that it should be a UV complete theory. While the spin-1 couplings automatically satisfy this, the pseudoscalar couplings (6.4) are dimension-5. We would thus like to consider renormalizable operators that generate (6.4). Because the SM fermions are chiral, there are no renormalizable interactions with the SM singlet  $\varphi$  and the SM fermions. We thus left with

interactions between the Higgs and the pseudoscalar,

$$\mathcal{L}_{\varphi H} = |H|^2 \lambda_H (M\varphi + \varphi^2), \quad (6.5)$$

where  $M$  is a dimensionful coupling. These couplings are reminiscent of the Higgs portal framework [177, 178] with the caveat that  $\varphi$  is now a mediator rather than the DM particle. At energies below  $m_h$ , (6.5) generates the couplings in (6.4) with the prediction  $\lambda_u = \lambda_d = \lambda_\ell$ . This is model dependent: In a two-Higgs doublet model such as the MSSM, one may have  $\varphi$  mix differently with the up- and down-type Higgses. These couplings introduce additional handles for dark sector bounds through the invisible width of the Higgs. See [179] for an explicit model for the  $\gamma$ -ray excess of this type.

## 6.4 Self-Interacting Dark Matter

The on-shell mediator scenario has nontrivial dynamics even in the limit of parametrically small coupling to the SM and may be a candidate for a model of self-interacting dark matter. However, the lower bound on the mediator mass (2.4d) is heavier than the typical scale required to address anomalies in small-scale structure [88, 91, 92, 97, 99–102, 105–107, 180, 181]. A complete study of DM self-interactions through a pseudoscalar has yet to be completed, though the first steps are presented in [89] and have indicated that resonance effects may be relevant even for  $m_\varphi \gtrsim 10$  GeV. Alternately, in Appendix A we address alternate final states that may match the  $\gamma$ -ray excess. Of particular interest is a mediator which decays into gluons—say through a loop of heavy quarks—could be made light enough to plausibly be in the regime of interesting models for self-interaction. We leave a detailed exploration for future work.

## 6.5 Prototypes for UV models

We briefly comment on directions in specific models that may be adapted to the on-shell mediator scenario. The MSSM introduces an additional pseudoscalar state which can plausibly mix with the Higgs as in (6.5), but SUSY bounds tend to rule out the mass range of interest. Alternately, the singlet superfield of the NMSSM may be sufficiently unconstrained to furnish the required pseudoscalar. More generally, [179] recently proposed a complete non-supersymmetric UV model with two-Higgs doublets for the  $\gamma$ -ray excess.

A second alternate direction is to develop models with spin-1 mediators. We have shown that these typically are forced to have a constrained SM coupling if the mediator has a universal coupling to all generations, as one may generically expect for a gauged symmetry; see [182] for an explicit leptophilic model. While a  $Z'$  coupling to  $U(1)_B$  and parametrically small coupling to the SM is a valid scenario within the on-shell mediator framework, one may also consider options where the spin-1 mediator does not have universal coupling, for example [183]. Inspiration for such a particle is motivated by Randall-Sundrum models [184] (gauge bosons with the 4D zero mode projected out, see e.g. [185, 186]) or their holographic duals (composite Higgs models with  $\rho$ -meson-like excitations) [187, 188].

## 6.6 Exceptions

Finally, we point out several exceptions to some of the ‘generic’ statements we have made in this document.

<b>Mediator</b>	<b>MASS [GeV]</b>		<b>INTERACTION</b>		<b>COUPLING</b>		<b>Thermal Relic?</b>
	$m_\chi$	$m_{\text{mes.}}$	<b>DM</b>	<b>SM</b>	$\lambda_{\text{DM}}$	$\lambda_{\text{SM}}$	
spin-0	110	20	$\gamma^5$	$\mathbb{1}$	1.2	$< 0.08$	MSP?
"	"	"	$\gamma^5$	$\gamma^5$	"	$< 0.02^*$	"
spin-1	45	14	$\gamma^\mu$	$\gamma_\mu$	0.18	$< 10^{-6}$	$\gamma = 1.3$
"	"	"	$\gamma^\mu \gamma^5$	$\gamma_\mu \gamma^5$	"	$< 0.004$	"
"	"	"	$\gamma^\mu \gamma^5$	$\gamma_\mu$	"	$< 0.006$	"
"	"	"	$\gamma^\mu$	$\gamma_\mu \gamma^5$	"	$< 0.02$	"

Table 3: Best fit parameters assuming  $b$ -philic couplings for the spin-0 mediator and universal quark couplings for the spin-1 mediator. The upper bound for  $\lambda_{\text{SM}}$  for the  $\gamma^5 \otimes \gamma^5$  is a conservative estimate for the 8 TeV mono- $b$  reach at the LHC (see Section 4.3); the other bounds come from direct detection. In the last column, we indicate whether consistency with a thermal relic abundance suggests a tighter DM profile ( $\gamma = 1.3$ ) or some population of millisecond pulsars (MSP), see Section 5.

- In Sec. 1.2 we motivated the on-shell mediator scenario by exploiting how bounds on one operator ‘generically’ bound others. Some of these bounds are avoided when  $\chi$  were a Majorana fermion since operators such as  $\bar{\chi}\gamma^\mu\chi \equiv 0$ . More generically one may also consider bosonic dark matter.
- In the MFV ansatz, we saw from the chiral structure that scalar couplings naturally follow the mass hierarchy while vector couplings tend to be universal. The latter condition is not necessary even within the MFV framework. For example, if the leading order spin-1 flavor spurion  $\delta_{ij}$  were to vanish, the next-to-leading term is  $y_i^\dagger y_j$  which has an even strongly hierarchical coupling to the third generation. Such a structure may be possible through models of partial compositeness [187, 188].
- We limited our analysis to a single class of mediator at a time. In the presence of multiple mediator fields, one can find processes that violate the relation between diagram topology and partial wave. For example,  $\chi\bar{\chi} \rightarrow \varphi_1\varphi_2$  is  $s$ -wave for distinct spin-0 particles  $\varphi_{1,2}$ .

## 7 Conclusions and Outlook

We have presented a class of simplified models where dark matter annihilates into on-shell mediators which, in turn, decay into the SM with a typically suppressed width. This separates the sector of the model which can account for indirect detection signals—such as the FERMI galactic center  $\gamma$ -ray excess—and those which are bounded by direct detection and collider experiments. We have addressed  $\gamma$ -ray spectrum coming from these models and have compared used the  $\gamma$ -ray excess to identify plausible regions of parameter space for a DM interpretation; the best fit parameters and bounds on the SM coupling are shown in Table 3. We have addressed the key points for UV model building and, in an appendix below, highlight further directions for modifying the  $\gamma$ -ray spectrum with more general SM final states.

## Acknowledgements

This work is supported in part by the NSF grant PHY-1316792. We thank Kev Abazajian, Nikhil Anand, Nicolas Canac, Eugenio Del Nobile, Jonathan Feng, Shunsaku Horiuchi, Manoj Kaplinghat, Gordan Krnjaic (*‘kern-ya-yitch’*), Tongyan Lin, Simona Murgia, Brian Shuve, Tracy Slatyer, Yuhsin Tsai, Daniel Whiteson, and Hai-Bo Yu for many insightful discussions. Plots in this document were generated using *Mathematica* [134]. P.T. would like to thank Southwest airlines and the airspace above the California coast where part of this work was completed.

While this paper was being prepared, [17, 118] was posted with an explicit model for on-shell vector mediators. [118] differs from the  $\chi\bar{\chi} \rightarrow VV$  mode in this work in that it examines a specific UV completion which includes semi-annihilations. Their  $1\sigma$  contours also do not account for the systematic uncertainties discussed in Sec. 3.3. Shortly after this work was posted to arXiv, [189] was posted and explores on-shell mediators with diverse SM final states and emphasizes the theme in our Figs. 10–8 and Appendix A that one need not focus only on bottom quark couplings and, further, that dark matter masses both above and below 40 GeV can yield the  $\gamma$ -ray excess.

## A The Spectrum of Spectra

In the main text we have shown how the conventional 40 GeV DM model for the  $\gamma$ -ray excess can be converted into a heavier DM model ( $m_\chi = 80, 120$  GeV) by taking the limit where annihilation to on-shell mediators dominates. We further showed that one can interpolate the DM masses between  $m_\chi = 40$  GeV and 80, 120 GeV by parametrically increasing the SM coupling and increasing the fraction annihilations through an off-shell mediator. In this appendix we briefly demonstrate nonstandard (i.e. beyond  $b\bar{b}$  and  $\tau\bar{\tau}$ ) spectra that may also fit the  $\gamma$ -ray excess in the regimes  $m_\chi < 40$  GeV and  $m_\chi > 80, 120$  GeV. We use PPPC as described in Sec. 3.2 and our fits are subject to the caveats described in Sec. 3.3. For simplicity and consistency when comparing to other plots in this paper, we plot the data fit to the  $b\bar{b}$  template from Fig. 8 of [13].

Fig. 11 shows sample spectra that show the range of behavior when considering different final states both for off-shell  $s$ -channel processes and for those with on-shell mediators. In each of these cases, we note that by considering either admixtures of different final states or on-shell mediator annihilation into different species, one can find viable DM models for the  $\gamma$ -ray excess where the DM mass is less than the 40 GeV value typically considered in the literature.

For example, we point out in (a) and (b) that gluons can give a reasonable fit to the spectrum. While the photon spectrum from monochromatic gluons takes a slightly different shape than that of the  $b$ —presumably part of the reason why  $gg$  final states were not proposed for the  $\gamma$ -ray excess fit—they are reasonably close to the data given the implicit systematic uncertainties. This fit is improved significantly if the [off-shell,  $s$ -channel] mediator is allowed to decay to both gluons or  $b\bar{b}$  pairs. Shown in (b) is the fit for a mediator that decays to either gluons or  $b\bar{b}$  pairs, with

$$\text{Br}(\text{mediator} \rightarrow gg) \approx 2 \text{Br}(\text{mediator} \rightarrow b\bar{b}). \quad (\text{A.1})$$

The gluon mode is especially amenable to lighter dark matter masses since the final state is massless. Couplings to a spin-0 mediator can be generated through, for example, loops of third generation quarks.

Similarly, in Fig. 11(c) we show what appears to be a poor fit to 10 GeV  $\tau\bar{\tau}$  pairs. This, however, is a consequence of comparing the  $\gamma$ -ray spectrum from  $\tau\bar{\tau}$  to the  $\gamma$ -ray excess fit assuming a  $b\bar{b}$

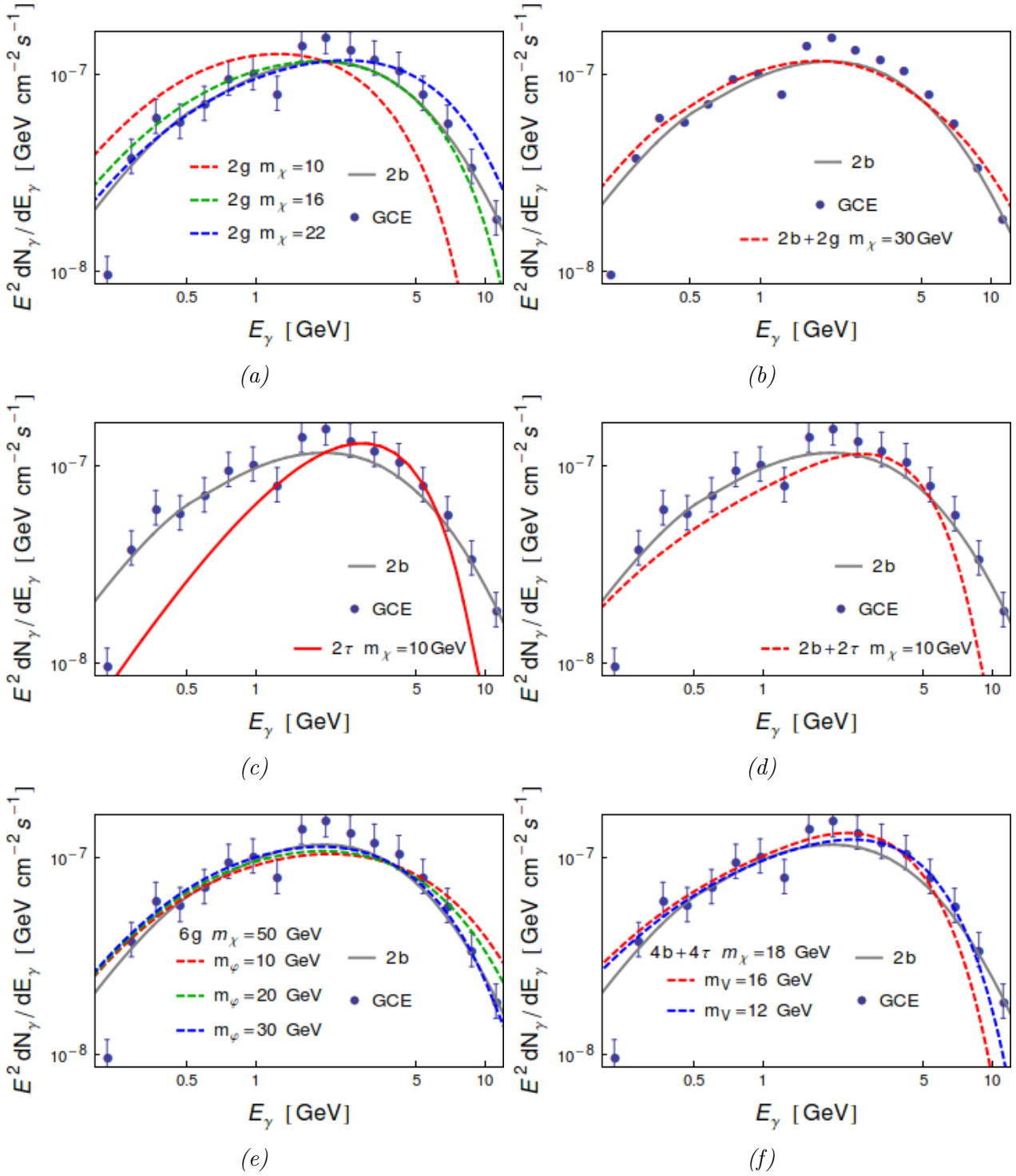


Figure 11: (a)  $\chi\bar{\chi} \rightarrow gg$ , (b)  $\chi\bar{\chi} \rightarrow gg$  (67%) or  $b\bar{b}$  (33%), (c)  $\chi\bar{\chi} \rightarrow \tau\bar{\tau}$ , (d)  $\chi\bar{\chi} \rightarrow \tau\bar{\tau}$  (85%) or  $b\bar{b}$  (15%), (e)  $\chi\bar{\chi} \rightarrow 6g$ , (f)  $\chi\bar{\chi} \rightarrow 2 \times [\tau\bar{\tau}$  (85%) or  $b\bar{b}$  (15%)]. Spectra for various final states, including branching ratios to different final states. 4-(6)-body final states originate from on-shell mediators with masses  $m_V$  ( $m_\phi$ ) shown. For visual comparison with other plots in this work, the gray 2b line is the  $\chi\bar{\chi} \rightarrow b\bar{b}$  best fit spectrum and dots are the measured galactic center  $\gamma$ -ray excess spectrum (GCE) assuming a  $b\bar{b}$  signal template from [13]. Bars demonstrate an arbitrary measure of goodness-of-fit with respect to this spectrum. Note that the  $\gamma$ -ray excess data depends on the template used for the DM  $\gamma$ -ray spectrum so these data points are mainly for comparative purposes and are not necessarily representative of the goodness-of-fit to the  $\gamma$ -ray excess. See Sec. 3.3 for details.

DM template. It is indeed well known that DM annihilating into 10 GeV  $\tau$ s fits the excess well; this should be taken as a reminder of the systematic uncertainties implicit with the  $\gamma$ -ray fits. It also serves to highlight that for a specific model, a proper assessment of the fit to the  $\gamma$  ray excess requires a full astrophysical fit to the specific annihilation mode (along the lines of [7] and [14]) where both the model parameters and background parameters are fit simultaneously. For our purposes here, we only highlight the change in the spectrum from (c) to (d) where we introduce a 15% branching ratio of the mediator going to  $b\bar{b}$ —the fit has interpolated between the two spectra and gives an intuitive handle for how to generate hybrid spectra. A similar hybrid spectrum was explored in Fig. 6 of [12].

In Fig. 11(e, f) we demonstrate the range of behavior for annihilation to on-shell mediators that each decay to either gluons or  $\tau\bar{\tau}/b\bar{b}$ . Note that an on-shell vector mediator cannot decay into two gluons by the Landau-Yang theorem so that one is forced to consider either  $\chi\bar{\chi} \rightarrow 2 \times (V \rightarrow ggg)$  or  $\chi\bar{\chi} \rightarrow 3 \times (\phi \rightarrow gg)$ , each with six final state gluons. We plot the latter case in (e). In (f) we see an example of an on-shell vector mediator that decays to  $\tau\bar{\tau}$  85% of the time and  $b\bar{b}$  the remainder. This spectrum fits the  $\gamma$ -ray excess spectrum for a  $b\bar{b}$  template with  $m_V \approx 12$  GeV.

Finally, we propose a simple extension where the DM mass can be made heavier than the region considered in the primary text. We saw that the on-shell mediator scenario raised the DM mass by having DM annihilation go into more final state primaries ( $b$  quarks). By extending the mediator sector to include additional on-shell states between the DM and SM sectors in Fig. 3, one may force larger dark matter masses. For example, [128] explored the cascade where  $\chi\bar{\chi} \rightarrow 2\phi_1$  with  $\phi_i \rightarrow 2\phi_{i+1}$  for the PAMELA positron excess [190]. See the appendix in that paper for analytical results for the generalization of the box spectrum to a higher polynomial spectrum where the degree of the polynomial is set by the number of on-shell mediator sectors. Additionally, as we mentioned above, one may use the Landau-Yang theorem to force  $V_1 \rightarrow 3g$  decays at the end of the cascade or use mediator sectors where symmetries force  $\phi_i \rightarrow n\phi_{i+1}$  with  $n > 2$ . We remember from our analysis in Sec. 5, however, that increasing the number of on-shell mediators per annihilation while maintaining the  $\gamma$ -ray excess signal also increases the annihilation cross section beyond what is expected from a simple thermal relic.

## References

- [1] S. Arrenberg, H. Baer, V. Barger, L. Baudis, D. Bauer, *et al.*, “Dark Matter in the Coming Decade: Complementary Paths to Discovery and Beyond,” [arXiv:1310.8621 \[hep-ph\]](#).
- [2] D. Hooper and T. R. Slatyer, “Two Emission Mechanisms in the Fermi Bubbles: a Possible Signal of Annihilating Dark Matter,” *Phys.Dark Univ.* **2** (2013) 118–138, [arXiv:1302.6589 \[astro-ph.HE\]](#).
- [3] N. Okada and O. Seto, “Gamma Ray Emission in Fermi Bubbles and Higgs Portal Dark Matter,” [arXiv:1310.5991 \[hep-ph\]](#).
- [4] W.-C. Huang, A. Urbano, and W. Xue, “Fermi Bubbles Under Dark Matter Scrutiny. Part I: Astrophysical Analysis,” [arXiv:1307.6862 \[hep-ph\]](#).
- [5] L. Goodenough and D. Hooper, “Possible Evidence for Dark Matter Annihilation in the Inner Milky Way from the Fermi Gamma Ray Space Telescope,” [arXiv:0910.2998 \[hep-ph\]](#).
- [6] D. Hooper and L. Goodenough, “Dark Matter Annihilation in the Galactic Center as Seen by the Fermi Gamma Ray Space Telescope,” *Phys.Lett.* **B697** (2011) 412–428, [arXiv:1010.2752 \[hep-ph\]](#).
- [7] K. N. Abazajian, “The Consistency of Fermi-Lat Observations of the Galactic Center with a Millisecond Pulsar Population in the Central Stellar Cluster,” *JCAP* **1103** (2011) 010, [arXiv:1011.4275 \[astro-ph.HE\]](#).
- [8] K. N. Abazajian and M. Kaplinghat, “Detection of a Gamma-Ray Source in the Galactic Center Consistent with Extended Emission from Dark Matter Annihilation and Concentrated Astrophysical Emission,” *Phys.Rev.* **D86** (2012) 083511, [arXiv:1207.6047 \[astro-ph.HE\]](#).
- [9] A. Boyarsky, D. Malyshev, and O. Ruchayskiy, “A Comment on the Emission from the Galactic Center as Seen by the Fermi Telescope,” *Phys.Lett.* **B705** (2011) 165–169, [arXiv:1012.5839 \[hep-ph\]](#).
- [10] D. Hooper and T. Linden, “On the Origin of the Gamma Rays from the Galactic Center,” *Phys.Rev.* **D84** (2011) 123005, [arXiv:1110.0006 \[astro-ph.HE\]](#).
- [11] C. Gordon and O. Macías, “Dark Matter and Pulsar Model Constraints from Galactic Center Fermi-Lat Gamma Ray Observations,” *Phys.Rev.* **D88** (2013) 083521, [arXiv:1306.5725 \[astro-ph.HE\]](#).
- [12] O. Macías and C. Gordon, “The Contribution of Cosmic Rays Interacting with Molecular Clouds to the Galactic Center Gamma-Ray Excess,” [arXiv:1312.6671 \[astro-ph.HE\]](#).



- [13] K. N. Abazajian, N. Canac, S. Horiuchi, and M. Kaplinghat, “Astrophysical and Dark Matter Interpretations of Extended Gamma-Ray Emission from the Galactic Center,” *Phys.Rev.* **D90** (2014) 023526, [arXiv:1402.4090 \[astro-ph.HE\]](#).
- [14] T. Daylan, D. P. Finkbeiner, D. Hooper, T. Linden, S. K. N. Portillo, *et al.*, “The Characterization of the Gamma-Ray Signal from the Central Milky Way: a Compelling Case for Annihilating Dark Matter,” [arXiv:1402.6703 \[astro-ph.HE\]](#).
- [15] K. P. Modak, D. Majumdar, and S. Rakshit, “A Possible Explanation of Low Energy  $\Gamma$ -Ray Excess from Galactic Centre and Fermi Bubble by a Dark Matter Model with Two Real Scalars,” [arXiv:1312.7488 \[hep-ph\]](#).
- [16] L. A. Anchordoqui and B. J. Vlcek, “W-Wimp Annihilation as a Source of the Fermi Bubbles,” *Phys.Rev.* **D88** (2013) 043513, [arXiv:1305.4625 \[hep-ph\]](#).
- [17] P. Ko, W.-I. Park, and Y. Tang, “Higgs Portal Vector Dark Matter for GeV Scale  $\gamma$ -Ray Excess from Galactic Center,” [arXiv:1404.5257 \[hep-ph\]](#).
- [18] M. R. Buckley, D. Hooper, and J. L. Rosner, “A Leptophobic Z’ and Dark Matter from Grand Unification,” *Phys.Lett.* **B703** (2011) 343–347, [arXiv:1106.3583 \[hep-ph\]](#).
- [19] M. Boucenna and S. Profumo, “Direct and Indirect Singlet Scalar Dark Matter Detection in the Lepton-Specific Two-Higgs-Doublet Model,” *Phys.Rev.* **D84** (2011) 055011, [arXiv:1106.3368 \[hep-ph\]](#).
- [20] G. Zhu, “Wimless Dark Matter and the Excess Gamma Rays from the Galactic Center,” *Phys.Rev.* **D83** (2011) 076011, [arXiv:1101.4387 \[hep-ph\]](#).
- [21] B. Kyae and J.-C. Park, “Light Dark Matter for Fermi-Lat and Cdms Observations,” *Phys.Lett.* **B732** (2014) 373–379, [arXiv:1310.2284 \[hep-ph\]](#).
- [22] G. Marshall and R. Primulando, “The Galactic Center Region Gamma Ray Excess from a Supersymmetric Leptophilic Higgs Model,” *JHEP* **1105** (2011) 026, [arXiv:1102.0492 \[hep-ph\]](#).
- [23] D. Cerdeno, M. Peiro, and S. Robles, “Low-Mass Right-Handed Sneutrino Dark Matter: Supercdms and Lux Constraints and the Galactic Centre Gamma-Ray Excess,” [arXiv:1404.2572 \[hep-ph\]](#).
- [24] P. Agrawal, B. Batell, D. Hooper, and T. Lin, “Flavored Dark Matter and the Galactic Center Gamma-Ray Excess,” [arXiv:1404.1373 \[hep-ph\]](#).
- [25] D. Hooper, I. Cholis, T. Linden, J. Siegal-Gaskins, and T. Slatyer, “Millisecond Pulsars Cannot Account for the Inner Galaxy’s GeV Excess,” *Phys.Rev.* **D88** (2013) 083009, [arXiv:1305.0830 \[astro-ph.HE\]](#).
- [26] Q. Yuan and B. Zhang, “Millisecond Pulsar Interpretation of the Galactic Center Gamma-Ray Excess,” [arXiv:1404.2318 \[astro-ph.HE\]](#).
- [27] M. Kaplinghat, *et al.* In Preparation.
- [28] K. Hagiwara, S. Mukhopadhyay, and J. Nakamura, “10 GeV Neutralino Dark Matter and Light Stau in the MSSM,” *Phys.Rev.* **D89** (2014) 015023, [arXiv:1308.6738 \[hep-ph\]](#).
- [29] M. R. Buckley, D. Hooper, and J. Kumar, “Phenomenology of Dirac Neutralino Dark Matter,” *Phys.Rev.* **D88** (2013) 063532, [arXiv:1307.3561](#).
- [30] H. E. Logan, “Dark Matter Annihilation Through a Lepton-Specific Higgs Boson,” *Phys.Rev.* **D83** (2011) 035022, [arXiv:1010.4214 \[hep-ph\]](#).
- [31] T. Lacroix, C. Boehm, and J. Silk, “Fitting the Fermi-Lat GeV Excess: on the Importance of Including the Propagation of Electrons from Dark Matter,” [arXiv:1403.1987 \[astro-ph.HE\]](#).
- [32] Q.-H. Cao, C.-R. Chen, C. S. Li, and H. Zhang, “Effective Dark Matter Model: Relic Density, Cdms II, Fermi Lat and Lhc,” *JHEP* **1108** (2011) 018, [arXiv:0912.4511 \[hep-ph\]](#).
- [33] M. Beltran, D. Hooper, E. W. Kolb, Z. A. Krusberg, and T. M. Tait, “Maverick Dark Matter at Colliders,” *JHEP* **1009** (2010) 037, [arXiv:1002.4137 \[hep-ph\]](#).
- [34] J. Goodman, M. Ibe, A. Rajaraman, W. Shepherd, T. M. Tait, *et al.*, “Constraints on Light Majorana Dark Matter from Colliders,” *Phys.Lett.* **B695** (2011) 185–188, [arXiv:1005.1286 \[hep-ph\]](#).
- [35] Y. Bai, P. J. Fox, and R. Harnik, “The Tevatron at the Frontier of Dark Matter Direct Detection,” *JHEP* **1012** (2010) 048, [arXiv:1005.3797 \[hep-ph\]](#).
- [36] J. Goodman, M. Ibe, A. Rajaraman, W. Shepherd, T. M. Tait, *et al.*, “Constraints on Dark Matter from Colliders,” *Phys.Rev.* **D82** (2010) 116010, [arXiv:1008.1783 \[hep-ph\]](#).
- [37] P. J. Fox, R. Harnik, J. Kopp, and Y. Tsai, “LEP Shines Light on Dark Matter,” *Phys.Rev.* **D84** (2011) 014028, [arXiv:1103.0240 \[hep-ph\]](#).
- [38] A. Rajaraman, W. Shepherd, T. M. Tait, and A. M. Wijangco, “Lhc Bounds on Interactions of Dark Matter,” *Phys.Rev.* **D84** (2011) 095013, [arXiv:1108.1196 \[hep-ph\]](#).
- [39] P. J. Fox, R. Harnik, J. Kopp, and Y. Tsai, “Missing Energy Signatures of Dark Matter at the Lhc,” *Phys.Rev.* **D85** (2012) 056011, [arXiv:1109.4398 \[hep-ph\]](#).
- [40] J.-F. Fortin and T. M. Tait, “Collider Constraints on Dipole-Interacting Dark Matter,” *Phys.Rev.* **D85** (2012) 063506, [arXiv:1103.3289 \[hep-ph\]](#).
- [41] N. F. Bell, J. B. Dent, A. J. Galea, T. D. Jacques, L. M. Krauss, *et al.*, “Searching for Dark Matter at the Lhc with a Mono-Z,” *Phys.Rev.* **D86** (2012) 096011, [arXiv:1209.0231 \[hep-ph\]](#).
- [42] K. Cheung, P.-Y. Tseng, Y.-L. S. Tsai, and T.-C. Yuan, “Global Constraints on Effective Dark Matter Interactions: Relic Density, Direct Detection, Indirect Detection, and Collider,” *JCAP* **1205** (2012) 001, [arXiv:1201.3402 \[hep-ph\]](#).
- [43] Y. Bai and T. M. Tait, “Searches with Mono-Leptons,” *Phys.Lett.* **B723** (2013) 384–387, [arXiv:1208.4361 \[hep-ph\]](#).
- [44] R. Ding and Y. Liao, “Spin 3/2 Particle as a Dark Matter Candidate: an Effective Field Theory Approach,” *JHEP* **1204** (2012) 054, [arXiv:1201.0506 \[hep-ph\]](#).
- [45] L. M. Carpenter, A. Nelson, C. Shimmin, T. M. Tait, and D. Whiteson, “Collider Searches for Dark Matter in Events with a Z Boson and Missing Energy,” *Phys.Rev.* **D87** (2013) no. 7, 074005, [arXiv:1212.3352](#).
- [46] R. Cotta, J. Hewett, M. Le, and T. Rizzo, “Bounds on Dark Matter Interactions with Electroweak Gauge Bosons,” *Phys.Rev.* **D88** (2013) 116009, [arXiv:1210.0525 \[hep-ph\]](#).
- [47] N. Zhou, D. Berge, and D. Whiteson, “Mono-Everything: Combined Limits on Dark Matter Production at Colliders from Multiple Final States,” *Phys.Rev.* **D87** (2013) no. 9, 095013, [arXiv:1302.3619 \[hep-ex\]](#).
- [48] L. Carpenter, A. DiFranzo, M. Mulhearn, C. Shimmin, S. Tulin, *et al.*, “Mono-Higgs: a New Collider Probe of Dark Matter,” [arXiv:1312.2592 \[hep-ph\]](#).
- [49] H. Dreiner, D. Schmeier, and J. Tattersall, “Contact Interactions Probe Effective Dark Matter Models at the Lhc,”

- Europhys.Lett.* **102** (2013) 51001, [arXiv:1303.3348 \[hep-ph\]](#).
- [50] T. Lin, E. W. Kolb, and L.-T. Wang, “Probing Dark Matter Couplings to Top and Bottom at the Lhc,” *Phys.Rev.* **D88** (2013) 063510, [arXiv:1303.6638 \[hep-ph\]](#).
  - [51] Z.-H. Yu, Q.-S. Yan, and P.-F. Yin, “Detecting Interactions Between Dark Matter and Photons at High Energy  $E^+E^-$  Colliders,” *arXiv:1307.5740 [hep-ph]*.
  - [52] A. Berlin, T. Lin, and L.-T. Wang, “Mono-Higgs Detection of Dark Matter at the Lhc,” [arXiv:1402.7074 \[hep-ph\]](#).
  - [53] M. Beltran, D. Hooper, E. W. Kolb, and Z. C. Krusberg, “Deducing the Nature of Dark Matter from Direct and Indirect Detection Experiments in the Absence of Collider Signatures of New Physics,” *Phys.Rev.* **D80** (2009) 043509, [arXiv:0808.3384 \[hep-ph\]](#).
  - [54] J. Goodman, M. Ibe, A. Rajaraman, W. Shepherd, T. M. Tait, *et al.*, “Gamma Ray Line Constraints on Effective Theories of Dark Matter,” *Nucl.Phys.* **B844** (2011) 55–68, [arXiv:1009.0008 \[hep-ph\]](#).
  - [55] K. Cheung, P.-Y. Tseng, and T.-C. Yuan, “Cosmic Antiproton Constraints on Effective Interactions of the Dark Matter,” *JCAP* **1101** (2011) 004, [arXiv:1011.2310 \[hep-ph\]](#).
  - [56] K. Cheung, P.-Y. Tseng, and T.-C. Yuan, “Gamma-Ray Constraints on Effective Interactions of the Dark Matter,” *JCAP* **1106** (2011) 023, [arXiv:1104.5329 \[hep-ph\]](#).
  - [57] A. Rajaraman, T. M. Tait, and A. M. Wijangco, “Effective Theories of Gamma-Ray Lines from Dark Matter Annihilation,” *Phys.Dark Univ.* **2** (2013) 17–21, [arXiv:1211.7061 \[hep-ph\]](#).
  - [58] A. De Simone, A. Monin, A. Thamm, and A. Urbano, “On the Effective Operators for Dark Matter Annihilations,” *JCAP* **1302** (2013) 039, [arXiv:1301.1486 \[hep-ph\]](#).
  - [59] J.-M. Zheng, Z.-H. Yu, J.-W. Shao, X.-J. Bi, Z. Li, *et al.*, “Constraining the Interaction Strength Between Dark Matter and Visible Matter: I. Fermionic Dark Matter,” *Nucl.Phys.* **B854** (2012) 350–374, [arXiv:1012.2022 \[hep-ph\]](#).
  - [60] A. Rajaraman, T. M. Tait, and D. Whiteson, “Two Lines Or Not Two Lines? That is the Question of Gamma Ray Spectra,” *JCAP* **1209** (2012) 003, [arXiv:1205.4723 \[hep-ph\]](#).
  - [61] G. Belanger, F. Boudjema, A. Pukhov, and A. Semenov, “Dark Matter Direct Detection Rate in a Generic Model with Micromegas 2.2,” *Comput.Phys.Commun.* **180** (2009) 747–767, [arXiv:0803.2360 \[hep-ph\]](#).
  - [62] A. Kurylov and M. Kamionkowski, “Generalized Analysis of Weakly Interacting Massive Particle Searches,” *Phys.Rev.* **D69** (2004) 063503, [arXiv:hep-ph/0307185 \[hep-ph\]](#).
  - [63] A. L. Fitzpatrick, W. Haxton, E. Katz, N. Lubbers, and Y. Xu, “Model Independent Direct Detection Analyses,” [arXiv:1211.2818 \[hep-ph\]](#).
  - [64] N. Anand, A. L. Fitzpatrick, and W. Haxton, “Model-Independent WIMP Scattering Responses and Event Rates: a Mathematica Package for Experimental Analysis,” [arXiv:1308.6288 \[hep-ph\]](#).
  - [65] J. Fan, M. Reece, and L.-T. Wang, “Non-Relativistic Effective Theory of Dark Matter Direct Detection,” *JCAP* **1011** (2010) 042, [arXiv:1008.1591 \[hep-ph\]](#).
  - [66] M. Freytsis and Z. Ligeti, “On Dark Matter Models with Uniquely Spin-Dependent Detection Possibilities,” *Phys.Rev.* **D83** (2011) 115009, [arXiv:1012.5317 \[hep-ph\]](#).
  - [67] T. Cohen, D. J. Phalen, and A. Pierce, “On the Correlation Between the Spin-Independent and Spin-Dependent Direct Detection of Dark Matter,” *Phys.Rev.* **D81** (2010) 116001, [arXiv:1001.3408 \[hep-ph\]](#).
  - [68] M. I. Gresham and K. M. Zurek, “On the Effect of Nuclear Response Functions in Dark Matter Direct Detection,” [arXiv:1401.3739 \[hep-ph\]](#).
  - [69] A. L. Fitzpatrick, W. Haxton, E. Katz, N. Lubbers, and Y. Xu, “The Effective Field Theory of Dark Matter Direct Detection,” *JCAP* **1302** (2013) 004, [arXiv:1203.3542 \[hep-ph\]](#).
  - [70] Y. Hochberg, E. Kuflik, T. Volansky, and J. G. Wacker, “The Simp Miracle,” [arXiv:1402.5143 \[hep-ph\]](#).
  - [71] D. Curtin, Z. Surujon, and Y. Tsai, “Direct Detection with Dark Mediators,” [arXiv:1312.2618 \[hep-ph\]](#).
  - [72] M. Papucci, A. Vichi, and K. M. Zurek, “Monojet Versus Rest of the World I: T-Channel Models,” [arXiv:1402.2285 \[hep-ph\]](#).
  - [73] J. Goodman and W. Shepherd, “LHC Bounds on UV-Complete Models of Dark Matter,” [arXiv:1111.2359 \[hep-ph\]](#).
  - [74] G. Busoni, A. De Simone, E. Morgante, and A. Riotto, “On the Validity of the Effective Field Theory for Dark Matter Searches at the Lhc,” *Phys.Lett.* **B728** (2014) 412–421, [arXiv:1307.2253 \[hep-ph\]](#).
  - [75] O. Buchmueller, M. J. Dolan, and C. McCabe, “Beyond Effective Field Theory for Dark Matter Searches at the Lhc,” *JHEP* **1401** (2014) 025, [arXiv:1308.6799 \[hep-ph\]](#).
  - [76] **LHC New Physics Working Group** Collaboration, D. Alves *et al.*, “Simplified Models for LHC New Physics Searches,” *J.Phys.* **G39** (2012) 105005, [arXiv:1105.2838 \[hep-ph\]](#).
  - [77] P. J. Fox and C. Williams, “Next-To-Leading Order Predictions for Dark Matter Production at Hadron Colliders,” *Phys.Rev.* **D87** (2013) no. 5, 054030, [arXiv:1211.6390 \[hep-ph\]](#).
  - [78] I. M. Shoemaker and L. Vecchi, “Unitarity and Monojet Bounds on Models for Dama, Cogent, and Cresst-Ii,” *Phys.Rev.* **D86** (2012) 015023, [arXiv:1112.5457 \[hep-ph\]](#).
  - [79] A. Friedland, M. L. Graesser, I. M. Shoemaker, and L. Vecchi, “Probing Nonstandard Standard Model Backgrounds with Lhc Monojets,” *Phys.Lett.* **B714** (2012) 267–275, [arXiv:1111.5331 \[hep-ph\]](#).
  - [80] M. L. Graesser, I. M. Shoemaker, and L. Vecchi, “A Dark Force for Baryons,” [arXiv:1107.2666 \[hep-ph\]](#).
  - [81] H. An, X. Ji, and L.-T. Wang, “Light Dark Matter and  $Z'$  Dark Force at Colliders,” *JHEP* **1207** (2012) 182, [arXiv:1202.2894 \[hep-ph\]](#).
  - [82] M. T. Frandsen, F. Kahlhoefer, A. Preston, S. Sarkar, and K. Schmidt-Hoberg, “Lhc and Tevatron Bounds on the Dark Matter Direct Detection Cross-Section for Vector Mediators,” *JHEP* **1207** (2012) 123, [arXiv:1204.3839 \[hep-ph\]](#).
  - [83] S. Profumo, W. Shepherd, and T. Tait, “The Pitfalls of Dark Crossings,” [arXiv:1307.6277 \[hep-ph\]](#).
  - [84] H. An, L.-T. Wang, and H. Zhang, “Dark Matter with T-Channel Mediator: a Simple Step Beyond Contact Interaction,” [arXiv:1308.0592 \[hep-ph\]](#).
  - [85] A. DiFranzo, K. I. Nagao, A. Rajaraman, and T. M. P. Tait, “Simplified Models for Dark Matter Interacting with Quarks,” *JHEP* **1311** (2013) 014, [arXiv:1308.2679 \[hep-ph\]](#).
  - [86] S. Chang, R. Edezhath, J. Hutchinson, and M. Luty, “Effective WIMPs,” *Phys.Rev.* **D89** (2014) 015011, [arXiv:1307.8120 \[hep-ph\]](#).
  - [87] R. C. Cotta, A. Rajaraman, T. M. P. Tait, and A. M. Wijangco, “Particle Physics Implications and Constraints on Dark Matter Interpretations of the CDMS Signal,” *Phys.Rev.* **D90** (2014) 013020, [arXiv:1305.6609 \[hep-ph\]](#).

- [88] M. Kaplinghat, S. Tulin, and H.-B. Yu, “Self-interacting Dark Matter Benchmarks,” [arXiv:1308.0618 \[hep-ph\]](#).
- [89] B. Bellazzini, M. Cliche, and P. Tanedo, “The Effective Theory of Self-Interacting Dark Matter,” *Phys.Rev.* **D88** (2013) 083506, [arXiv:1307.1129](#).
- [90] J. Fan, A. Katz, L. Randall, and M. Reece, “Double-Disk Dark Matter,” *Phys.Dark Univ.* **2** (2013) 139–156, [arXiv:1303.1521 \[astro-ph.CO\]](#).
- [91] S. Tulin, H.-B. Yu, and K. M. Zurek, “Beyond Collisionless Dark Matter: Particle Physics Dynamics for Dark Matter Halo Structure,” *Phys.Rev.* **D87** (2013) no. 11, 115007, [arXiv:1302.3898 \[hep-ph\]](#).
- [92] S. Tulin, H.-B. Yu, and K. M. Zurek, “Resonant Dark Forces and Small Scale Structure,” *Phys.Rev.Lett.* **110** (2013) no. 11, 111301, [arXiv:1210.0900 \[hep-ph\]](#).
- [93] F.-Y. Cyr-Racine and K. Sigurdson, “Cosmology of Atomic Dark Matter,” *Phys.Rev.* **D87** (2013) no. 10, 103515, [arXiv:1209.5752 \[astro-ph.CO\]](#).
- [94] R. Foot, “Implications of Mirror Dark Matter Kinetic Mixing for Cmb Anisotropies,” *Phys.Lett.* **B718** (2013) 745–751, [arXiv:1208.6022 \[astro-ph.CO\]](#).
- [95] S. Tulin, H.-B. Yu, and K. M. Zurek, “Three Exceptions for Thermal Dark Matter with Enhanced Annihilation to  $\Gamma\Gamma$ ,” *Phys.Rev.* **D87** (2013) 036011, [arXiv:1208.0009 \[hep-ph\]](#).
- [96] D. E. Kaplan, G. Z. Krnjaic, K. R. Rehermann, and C. M. Wells, “Dark Atoms: Asymmetry and Direct Detection,” *JCAP* **1110** (2011) 011, [arXiv:1105.2073 \[hep-ph\]](#).
- [97] A. Loeb and N. Weiner, “Cores in Dwarf Galaxies from Dark Matter with a Yukawa Potential,” *Phys.Rev.Lett.* **106** (2011) 171302, [arXiv:1011.6374 \[astro-ph.CO\]](#).
- [98] H. An, S.-L. Chen, R. N. Mohapatra, and Y. Zhang, “Leptogenesis as a Common Origin for Matter and Dark Matter,” *JHEP* **1003** (2010) 124, [arXiv:0911.4463 \[hep-ph\]](#).
- [99] M. R. Buckley and P. J. Fox, “Dark Matter Self-Interactions and Light Force Carriers,” *Phys.Rev.* **D81** (2010) 083522, [arXiv:0911.3898 \[hep-ph\]](#).
- [100] J. L. Feng, M. Kaplinghat, and H.-B. Yu, “Halo Shape and Relic Density Exclusions of Sommerfeld-Enhanced Dark Matter Explanations of Cosmic Ray Excesses,” *Phys.Rev.Lett.* **104** (2010) 151301, [arXiv:0911.0422 \[hep-ph\]](#).
- [101] J. L. Feng, M. Kaplinghat, H. Tu, and H.-B. Yu, “Hidden Charged Dark Matter,” *JCAP* **0907** (2009) 004, [arXiv:0905.3039 \[hep-ph\]](#).
- [102] M. Pospelov and A. Ritz, “Astrophysical Signatures of Secluded Dark Matter,” *Phys.Lett.* **B671** (2009) 391–397, [arXiv:0810.1502 \[hep-ph\]](#).
- [103] N. Arkani-Hamed, D. P. Finkbeiner, T. R. Slatyer, and N. Weiner, “A Theory of Dark Matter,” *Phys.Rev.* **D79** (2009) 015014, [arXiv:0810.0713 \[hep-ph\]](#).
- [104] M. Kesden and M. Kamionkowski, “Galilean Equivalence for Galactic Dark Matter,” *Phys.Rev.Lett.* **97** (2006) 131303, [arXiv:astro-ph/0606566 \[astro-ph\]](#).
- [105] R. Foot, “Mirror Matter-Type Dark Matter,” *Int.J.Mod.Phys.* **D13** (2004) 2161–2192, [arXiv:astro-ph/0407623 \[astro-ph\]](#).
- [106] R. Mohapatra, S. Nussinov, and V. Teplitz, “Mirror Matter as Selfinteracting Dark Matter,” *Phys.Rev.* **D66** (2002) 063002, [arXiv:hep-ph/0111381 \[hep-ph\]](#).
- [107] D. N. Spergel and P. J. Steinhardt, “Observational Evidence for Selfinteracting Cold Dark Matter,” *Phys.Rev.Lett.* **84** (2000) 3760–3763, [arXiv:astro-ph/9909386 \[astro-ph\]](#).
- [108] A. Alves, S. Profumo, F. S. Queiroz, and W. Shepherd, “The Effective Hooperon,” [arXiv:1403.5027 \[hep-ph\]](#).
- [109] **LUX Collaboration** Collaboration, D. Akerib *et al.*, “First Results from the Lux Dark Matter Experiment at the Sanford Underground Research Facility,” [arXiv:1310.8214 \[astro-ph.CO\]](#).
- [110] **XENON100 Collaboration** Collaboration, E. Aprile *et al.*, “Limits on Spin-Dependent Wimp-Nucleon Cross Sections from 225 Live Days of Xenon100 Data,” *Phys.Rev.Lett.* **111** (2013) no. 2, 021301, [arXiv:1301.6620 \[astro-ph.CO\]](#).
- [111] **ATLAS Collaboration** Collaboration, “Search for New Phenomena in Monojet plus Missing Transverse Momentum Final States using  $10\text{fb}^{-1}$  of pp Collisions at  $\sqrt{s} = 8$  TeV with the ATLAS detector at the LHC,” Tech. Rep. ATLAS-CONF-2012-147, CERN, Geneva, Nov, 2012.
- [112] W.-C. Huang, A. Urbano, and W. Xue, “Fermi Bubbles Under Dark Matter Scrutiny Part II: Particle Physics Analysis,” [arXiv:1310.7609 \[hep-ph\]](#).
- [113] A. Berlin, D. Hooper, and S. D. McDermott, “Simplified Dark Matter Models for the Galactic Center Gamma-Ray Excess,” [arXiv:1404.0022 \[hep-ph\]](#).
- [114] E. Izaguirre, G. Krnjaic, and B. Shuve, “The Galactic Center Excess from the Bottom Up,” [arXiv:1404.2018 \[hep-ph\]](#).
- [115] C. Boehm, M. J. Dolan, C. McCabe, M. Spannowsky, and C. J. Wallace, “Extended Gamma-Ray Emission from Coy Dark Matter,” [arXiv:1401.6458 \[hep-ph\]](#).
- [116] A. Hektor and L. Marzola, “Coy Dark Matter and the Anomalous Magnetic Moment,” [arXiv:1403.3401 \[hep-ph\]](#).
- [117] F. D’Eramo and J. Thaler, “Semi-annihilation of Dark Matter,” *JHEP* **1006** (2010) 109, [arXiv:1003.5912 \[hep-ph\]](#).
- [118] C. Boehm, M. J. Dolan, and C. McCabe, “A weighty interpretation of the Galactic Centre excess,” *Phys.Rev.* **D90** (2014) 023531, [arXiv:1404.4977 \[hep-ph\]](#).
- [119] H. K. Dreiner, H. E. Haber, and S. P. Martin, “Two-Component Spinor Techniques and Feynman Rules for Quantum Field Theory and Supersymmetry,” *Phys.Rept.* **494** (2010) 1–196, [arXiv:0812.1594 \[hep-ph\]](#).
- [120] J. Kumar and D. Marfatia, “Matrix Element Analyses of Dark Matter Scattering and Annihilation,” *Phys.Rev.* **D88** (2013) 014035, [arXiv:1305.1611 \[hep-ph\]](#).
- [121] L. Hall and L. Randall, “Weak Scale Effective Supersymmetry,” *Phys.Rev.Lett.* **65** (1990) 2939–2942.
- [122] R. S. Chivukula and H. Georgi, “Composite Technicolor Standard Model,” *Phys.Lett.* **B188** (1987) 99.
- [123] A. Buras, P. Gambino, M. Gorbahn, S. Jager, and L. Silvestrini, “Universal Unitarity Triangle and Physics Beyond the Standard Model,” *Phys.Lett.* **B500** (2001) 161–167, [arXiv:hep-ph/0007085 \[hep-ph\]](#).
- [124] G. D’Ambrosio, G. Giudice, G. Isidori, and A. Strumia, “Minimal Flavor Violation: an Effective Field Theory Approach,” *Nucl.Phys.* **B645** (2002) 155–187, [arXiv:hep-ph/0207036 \[hep-ph\]](#).
- [125] J. F. Navarro, C. S. Frenk, and S. D. White, “The Structure of Cold Dark Matter Halos,” *Astrophys.J.* **462** (1996) 563–575, [arXiv:astro-ph/9508025 \[astro-ph\]](#).
- [126] J. F. Navarro, C. S. Frenk, and S. D. White, “A Universal Density Profile from Hierarchical Clustering,” *Astrophys.J.* **490** (1997) 493–508, [arXiv:astro-ph/9611107 \[astro-ph\]](#).

- [127] A. Klypin, H. Zhao, and R. S. Somerville, “Lambda Cdm-Based Models for the Milky Way and M31 I: Dynamical Models,” *Astrophys.J.* **573** (2002) 597–613, [arXiv:astro-ph/0110390 \[astro-ph\]](#).
- [128] J. Mardon, Y. Nomura, D. Stolarski, and J. Thaler, “Dark Matter Signals from Cascade Annihilations,” *JCAP* **0905** (2009) 016, [arXiv:0901.2926 \[hep-ph\]](#).
- [129] A. Ibarra, S. Lopez Gehler, and M. Pato, “Dark Matter Constraints from Box-Shaped Gamma-Ray Features,” *JCAP* **1207** (2012) 043, [arXiv:1205.0007 \[hep-ph\]](#).
- [130] J. Alwall, M. Herquet, F. Maltoni, O. Mattelaer, and T. Stelzer, “Madgraph 5 : Going Beyond,” *JHEP* **1106** (2011) 128, [arXiv:1106.0522 \[hep-ph\]](#).
- [131] M. Cirelli, “PPPC 4 DM ID - A Poor Particle Physicist Cookbook for Dark Matter Indirect Detection,” December, 2013. <http://www.marcocirelli.net/PPPC4DMID.html>.
- [132] M. Cirelli, G. Corcella, A. Hektor, G. Hutsi, M. Kadastik, *et al.*, “PPPC 4 DM ID: a Poor Particle Physicist Cookbook for Dark Matter Indirect Detection,” *JCAP* **1103** (2011) 051, [arXiv:1012.4515 \[hep-ph\]](#).
- [133] P. Ciafaloni, D. Comelli, A. Riotto, F. Sala, A. Strumia, *et al.*, “Weak Corrections are Relevant for Dark Matter Indirect Detection,” *JCAP* **1103** (2011) 019, [arXiv:1009.0224 \[hep-ph\]](#).
- [134] Wolfram Research, Inc., *Mathematica, Version 8.0*. Champaign, Illinois, 2010.
- [135] T. Sjostrand, S. Mrenna, and P. Z. Skands, “A Brief Introduction to Pythia 8.1,” *Comput.Phys.Commun.* **178** (2008) 852–867, [arXiv:0710.3820 \[hep-ph\]](#).
- [136] M. Cirelli and G. Giesen, “Antiprotons from Dark Matter: Current Constraints and Future Sensitivities,” *JCAP* **1304** (2013) 015, [arXiv:1301.7079 \[hep-ph\]](#).
- [137] K. Kong and J.-C. Park, “Bounds on Dark Matter Interpretation of Fermi-Lat GeV Excess,” [arXiv:1404.3741 \[hep-ph\]](#).
- [138] **XENON100 Collaboration** Collaboration, E. Aprile *et al.*, “Dark Matter Results from 225 Live Days of Xenon100 Data,” *Phys.Rev.Lett.* **109** (2012) 181301, [arXiv:1207.5988 \[astro-ph.CO\]](#).
- [139] J. Kopp, V. Niro, T. Schwetz, and J. Zupan, “Dama/Libra and Leptonically Interacting Dark Matter,” *Phys.Rev.* **D80** (2009) 083502, [arXiv:0907.3159 \[hep-ph\]](#).
- [140] M. I. Gresham and K. M. Zurek, “Light Dark Matter Anomalies After Lux,” *Phys.Rev.* **D89** (2014) 016017, [arXiv:1311.2082 \[hep-ph\]](#).
- [141] M. Cirelli, E. Del Nobile, and P. Panci, “Tools for Model-Independent Bounds in Direct Dark Matter Searches,” *JCAP* **1310** (2013) 019, [arXiv:1307.5955 \[hep-ph\]](#).
- [142] B. A. Dobrescu and F. Yu, “Coupling-Mass Mapping of Dijet Peak Searches,” *Phys.Rev.* **D88** (2013) no. 3, 035021, [arXiv:1306.2629 \[hep-ph\]](#).
- [143] C. D. Carone and H. Murayama, “Possible light U(1) gauge boson coupled to baryon number,” *Phys.Rev.Lett.* **74** (1995) 3122–3125, [arXiv:hep-ph/9411256 \[hep-ph\]](#).
- [144] C. D. Carone and H. Murayama, “Realistic Models with a Light U(1) Gauge Boson Coupled to Baryon Number,” *Phys.Rev.* **D52** (1995) 484–493, [arXiv:hep-ph/9501220 \[hep-ph\]](#).
- [145] M. Williams, C. Burgess, A. Maharana, and F. Quevedo, “New Constraints (And Motivations) for Abelian Gauge Bosons in the MeV-Tev Mass Range,” *JHEP* **1108** (2011) 106, [arXiv:1103.4556 \[hep-ph\]](#).
- [146] B. A. Dobrescu and C. Frugiuale, “Hidden GeV-Scale Interactions of Quarks,” [arXiv:1404.3947 \[hep-ph\]](#).
- [147] D. Whiteson, *et al.* Private Communication.
- [148] M. Srednicki, R. Watkins, and K. A. Olive, “Calculations of Relic Densities in the Early Universe,” *Nucl.Phys.* **B310** (1988) 693.
- [149] E. Kolb and M. Turner, *The Early Universe*. Westview Press, 1994.
- [150] **WMAP Collaboration** Collaboration, J. Dunkley *et al.*, “Five-Year Wilkinson Microwave Anisotropy Probe (Wmap) Observations: Likelihoods and Parameters from the WMAP Data,” *Astrophys.J.Suppl.* **180** (2009) 306–329, [arXiv:0803.0586 \[astro-ph\]](#).
- [151] **WMAP Collaboration** Collaboration, E. Komatsu *et al.*, “Five-Year Wilkinson Microwave Anisotropy Probe (Wmap) Observations: Cosmological Interpretation,” *Astrophys.J.Suppl.* **180** (2009) 330–376, [arXiv:0803.0547 \[astro-ph\]](#).
- [152] **Planck Collaboration** Collaboration, P. Ade *et al.*, “Planck 2013 results. I. Overview of products and scientific results,” [arXiv:1303.5062 \[astro-ph.CO\]](#).
- [153] M. Pierre, J. M. Siegal-Gaskins, and P. Scott, “Sensitivity of Cta to Dark Matter Signals from the Galactic Center,” [arXiv:1401.7330 \[astro-ph.HE\]](#).
- [154] K. M. Zurek, “Asymmetric Dark Matter: Theories, Signatures, and Constraints,” *Phys.Rept.* **537** (2014) 91–121, [arXiv:1308.0338 \[hep-ph\]](#).
- [155] R. Easther, R. Galvez, O. Ozsoy, and S. Watson, “Supersymmetry, Nonthermal Dark Matter and Precision Cosmology,” *Phys.Rev.* **D89** (2014) 023522, [arXiv:1307.2453 \[hep-ph\]](#).
- [156] K. Petraki and R. R. Volkas, “Review of Asymmetric Dark Matter,” *Int.J.Mod.Phys.* **A28** (2013) 1330028, [arXiv:1305.4939 \[hep-ph\]](#).
- [157] J. McDonald, “Comment on the ‘Freeze-In’ Mechanism of Dark Matter Production,” [arXiv:1112.1501 \[hep-ph\]](#).
- [158] G. Arcadi and P. Ullio, “Accurate Estimate of the Relic Density and the Kinetic Decoupling in Non-Thermal Dark Matter Models,” *Phys.Rev.* **D84** (2011) 043520, [arXiv:1104.3591 \[hep-ph\]](#).
- [159] P. Sandick and S. Watson, “Constraints on a Non-Thermal History from Galactic Dark Matter Spikes,” *Phys.Rev.* **D84** (2011) 023507, [arXiv:1102.2897 \[astro-ph.CO\]](#).
- [160] L. J. Hall, K. Jedamzik, J. March-Russell, and S. M. West, “Freeze-In Production of Fimp Dark Matter,” *JHEP* **1003** (2010) 080, [arXiv:0911.1120 \[hep-ph\]](#).
- [161] R. Aloisio, V. Berezhinsky, and M. Kachelriess, “On the Status of Superheavy Dark Matter,” *Phys.Rev.* **D74** (2006) 023516, [arXiv:astro-ph/0604311 \[astro-ph\]](#).
- [162] J. L. Feng, S.-f. Su, and F. Takayama, “Superwimp Gravitino Dark Matter from Slepton and Sneutrino Decays,” *Phys.Rev.* **D70** (2004) 063514, [arXiv:hep-ph/0404198 \[hep-ph\]](#).
- [163] J. L. Feng, A. Rajaraman, and F. Takayama, “Superwimp Dark Matter Signals from the Early Universe,” *Phys.Rev.* **D68** (2003) 063504, [arXiv:hep-ph/0306024 \[hep-ph\]](#).
- [164] J. L. Feng, A. Rajaraman, and F. Takayama, “Superweakly Interacting Massive Particles,” *Phys.Rev.Lett.* **91** (2003) 011302, [arXiv:hep-ph/0302215 \[hep-ph\]](#).
- [165] E. A. Baltz and H. Murayama, “Gravitino Warm Dark Matter with Entropy Production,” *JHEP* **0305** (2003) 067,



- [arXiv:astro-ph/0108172](#) [[astro-ph](#)].
- [166] J. McDonald, “Thermally Generated Gauge Singlet Scalars as Selfinteracting Dark Matter,” *Phys.Rev.Lett.* **88** (2002) 091304, [arXiv:hep-ph/0106249](#) [[hep-ph](#)].
  - [167] E. W. Kolb, D. J. Chung, and A. Riotto, “Wimpzillas!,” [arXiv:hep-ph/9810361](#) [[hep-ph](#)].
  - [168] D. J. Chung, E. W. Kolb, and A. Riotto, “Production of Massive Particles during Reheating,” *Phys.Rev.* **D60** (1999) 063504, [arXiv:hep-ph/9809453](#) [[hep-ph](#)].
  - [169] D. J. Chung, E. W. Kolb, and A. Riotto, “Superheavy Dark Matter,” *Phys.Rev.* **D59** (1998) 023501, [arXiv:hep-ph/9802238](#) [[hep-ph](#)].
  - [170] L. Kofman, A. D. Linde, and A. A. Starobinsky, “Reheating After Inflation,” *Phys.Rev.Lett.* **73** (1994) 3195–3198, [arXiv:hep-th/9405187](#) [[hep-th](#)].
  - [171] J. R. Ellis, G. Gelmini, J. L. Lopez, D. V. Nanopoulos, and S. Sarkar, “Astrophysical Constraints on Massive Unstable Neutral Relic Particles,” *Nucl.Phys.* **B373** (1992) 399–437.
  - [172] J. R. Ellis, D. V. Nanopoulos, and S. Sarkar, “The Cosmology of Decaying Gravitinos,” *Nucl.Phys.* **B259** (1985) 175.
  - [173] N. Mirabal, “Dark Matter Vs. Pulsars: Catching the Impostor,” [arXiv:1309.3428](#) [[astro-ph.HE](#)].
  - [174] R. Voss and M. Gilfanov, “Dynamical Formation of X-Ray Binaries in the Inner Bulge of M31,” [arXiv:astro-ph/0702580](#) [[ASTRO-PH](#)].
  - [175] B. Batell, J. Pradler, and M. Spannowsky, “Dark Matter from Minimal Flavor Violation,” *JHEP* **1108** (2011) 038, [arXiv:1105.1781](#) [[hep-ph](#)].
  - [176] P. Agrawal, M. Blanke, and K. Gemmler, “Flavored dark matter beyond Minimal Flavor Violation,” [arXiv:1405.6709](#) [[hep-ph](#)].
  - [177] V. Silveira and A. Zee, “Scalar Phantoms,” *Phys.Lett.* **B161** (1985) 136.
  - [178] B. Patt and F. Wilczek, “Higgs-Field Portal into Hidden Sectors,” [arXiv:hep-ph/0605188](#) [[hep-ph](#)].
  - [179] S. Ipek, D. McKeen, and A. E. Nelson, “A Renormalizable Model for the Galactic Center Gamma Ray Excess from Dark Matter Annihilation,” [arXiv:1404.3716](#) [[hep-ph](#)].
  - [180] S. Tulin, “New Weakly-Coupled Forces Hidden in Low-Energy QCD,” [arXiv:1404.4370](#) [[hep-ph](#)].
  - [181] M. Kaplinghat, S. Tulin, and H.-B. Yu, “Direct Detection Portals for Self-Interacting Dark Matter,” *Phys.Rev.* **D89** (2014) 035009, [arXiv:1310.7945](#) [[hep-ph](#)].
  - [182] D. Hooper, N. Weiner, and W. Xue, “Dark Forces and Light Dark Matter,” *Phys.Rev.* **D86** (2012) 056009, [arXiv:1206.2929](#) [[hep-ph](#)].
  - [183] C. D. Carone, “Flavor-Nonuniversal Dark Gauge Bosons and the Muon G-2,” *Phys.Lett.* **B721** (2013) 118–122, [arXiv:1301.2027](#) [[hep-ph](#)].
  - [184] L. Randall and R. Sundrum, “A Large Mass Hierarchy from a Small Extra Dimension,” *Phys.Rev.Lett.* **83** (1999) 3370–3373, [arXiv:hep-ph/9905221](#) [[hep-ph](#)].
  - [185] L. Randall and M. D. Schwartz, “Quantum Field Theory and Unification in AdS5,” *JHEP* **0111** (2001) 003, [arXiv:hep-th/0108114](#) [[hep-th](#)].
  - [186] C. Csaki, J. Erlich, and J. Terning, “The Effective Lagrangian in the Randall-Sundrum Model and Electroweak Physics,” *Phys.Rev.* **D66** (2002) 064021, [arXiv:hep-ph/0203034](#) [[hep-ph](#)].
  - [187] R. Contino, D. Marzocca, D. Pappadopulo, and R. Rattazzi, “On the Effect of Resonances in Composite Higgs Phenomenology,” *JHEP* **1110** (2011) 081, [arXiv:1109.1570](#) [[hep-ph](#)].
  - [188] B. Bellazzini, C. Csaki, J. Hubisz, J. Serra, and J. Terning, “Composite Higgs Sketch,” *JHEP* **1211** (2012) 003, [arXiv:1205.4032](#) [[hep-ph](#)].
  - [189] A. Martin, J. Shelton, and J. Unwin, “Fitting the Galactic Center Gamma-Ray Excess with Cascade Annihilations,” [arXiv:1405.0272](#) [[hep-ph](#)].
  - [190] **PAMELA Collaboration** Collaboration, O. Adriani *et al.*, “An Anomalous Positron Abundance in Cosmic Rays with Energies 1.5-100 GeV,” *Nature* **458** (2009) 607–609, [arXiv:0810.4995](#) [[astro-ph](#)].